Theory of Decay of Superfluid Turbulence in the Low-Temperature Limit

Author(s):
Kozik, Evgeny V.; Svistunov, Boris V.

Publication date:
2009-09

Permanent link:
https://doi.org/10.3929/ethz-b-000016157

Originally published in:
Journal of Low Temperature Physics 156(3-6), https://doi.org/10.1007/s10909-009-9914-y

J Low Temp Phys (2009) 156: 215–267
DOI 10.1007/s10909-009-9914-y

Theory of Decay of Superfluid Turbulence in the Low-Temperature Limit

E.V. Kozik · B.V. Svistunov

Received: 8 April 2009 / Accepted: 30 June 2009 / Published online: 28 July 2009

Abstract We review the theory of relaxational kinetics of superfluid turbulence—a tangle of quantized vortex lines—in the limit of very low temperatures when the motion of vortices is conservative. While certain important aspects of the decay kinetics depend on whether the tangle is non-structured, like the one corresponding to the Kibble-Zurek picture, or essentially polarized, like the one that emulates the Richardson-Kolmogorov regime of classical turbulence, there are common fundamental features. In both cases, there exists an asymptotic range in the wavenumber space where the energy flux is supported by the cascade of Kelvin waves (kelvons)—precessing distortions propagating along the vortex filaments.

At large enough wavenumbers, the Kelvin-wave cascade is supported by three-kelvon elastic scattering. At zero temperature, the dissipative cutoff of the Kelvin-wave cascade is due to the emission of phonons, in which an elementary process converts two kelvons with almost opposite momenta into one bulk phonon.

Along with the standard set of conservation laws, a crucial role in the theory of low-temperature vortex dynamics is played by the fact of integrability of the local induction approximation (LIA) controlled by the parameter $\Lambda = \ln(\lambda/a_0)$, with λ the characteristic kelvon wavelength and a_0 the vortex core radius. While excluding a straightforward onset of the pure three-kelvon cascade, the integrability of LIA does not plug the cascade because of the natural availability of the kinetic channels associated with vortex line reconnections.

E.V. Kozik (✉)
Theoretische Physik, ETH Zürich, 8093 Zürich, Switzerland
e-mail: kozik@phys.ethz.ch

B.V. Svistunov
Department of Physics, University of Massachusetts, Amherst, MA 01003, USA

B.V. Svistunov
Russian Research Center “Kurchatov Institute”, 123182 Moscow, Russia

We argue that the crossover from Richardson-Kolmogorov to the Kelvin-wave cascade is due to eventual dominance of local induction of a single line over the collective induction of polarized eddies, which causes the breakdown of classical-fluid regime and gives rise to a reconnection-driven inertial range.

Keywords Vortex dynamics · Turbulence · Kelvin-wave cascade

1 Introduction

Superfluid turbulence (ST), also known as quantum/quantized turbulence, is a tangle of quantized vortex lines in a superfluid [1–4]. In the last one and a half decade, and especially in the recent years, the problem of *zero-point* ST has evolved into a really hot subfield of low-temperature physics [5–31]. In this work, we summarize theoretical developments of the two authors on the theory of decay of ST at $T = 0$, previously published in a number of short papers/letters [13–15, 20, 22]. To render the discussion self-contained, we also review the analysis of Ref. [5], where a number of conceptually important facts about zero-point ST has been revealed. We explicitly confine ourselves to the fundamental case of homogeneous isotropic turbulence occupying a large volume, which allows us to ignore influence of the boundary effects and possible tangle diffusion discussed elsewhere [25, 29].

Superfluid turbulence (ST) can be created in a number of ways: (i) in the counter-flow of normal and superfluid components [32–36, 40] (ii) by vibrating objects [7, 16, 17, 27], (iii) as a result of macroscopic motion of a superfluid (referred to as *quasi-classical* turbulence), in which case ST can mimic, at large enough length scales, classical-fluid turbulence [6, 16, 18, 23, 37–39], (iv) by the recently developed technique of ion injection [23], (v) in the process of (strongly) non-equilibrium Bose-Einstein condensation [41, 42], in which case it is a manifestation of generic Kibble-Zurek effect [43, 44], (vi) by an external perturbation of the trap in atomic Bose-Einstein condensates [30], etc.

During about four decades—from mid fifties till mid nineties—ST turbulence was intensively studied in the context of counter-flow of normal and superfluid components. An impressive success has been achieved in the field, with the prominent contributions by Vinen—the equation for qualitative description of growth/ decay kinetics (Vinen's equation), extensive experimental studies [32–34],—and pioneering microscopic simulations of vortex line dynamics by Schwartz [35, 36]. The counter-flow setup naturally implies finite density of the normal component, and thus a relatively simple—by comparison with the $T = 0$ case—relaxation mechanism. The normal component exerts a drag force on a vortex filament. As a result, the vortex line length decreases. For an illustration, consider a vortex circle of the radius R. In the absence of normal component, the ring moves with a constant velocity $V \equiv V(R)$, the radius R remaining constant. With the drag force, the ring collapses, obeying a simple law $\dot{R} \propto -\alpha V(R)$, where α is the dimensionless friction coefficient measuring the drag force in the units of Magnus force. Similarly, the drag causes the decay of Kelvin waves—precessing distortions on the vortex filaments—and the value of α^{-1} gives the number of revolutions a distortion makes before its amplitude significantly decreases. At $\alpha \sim 1$, the decay scenario of a (non-structured) vortex tangle is as follows.

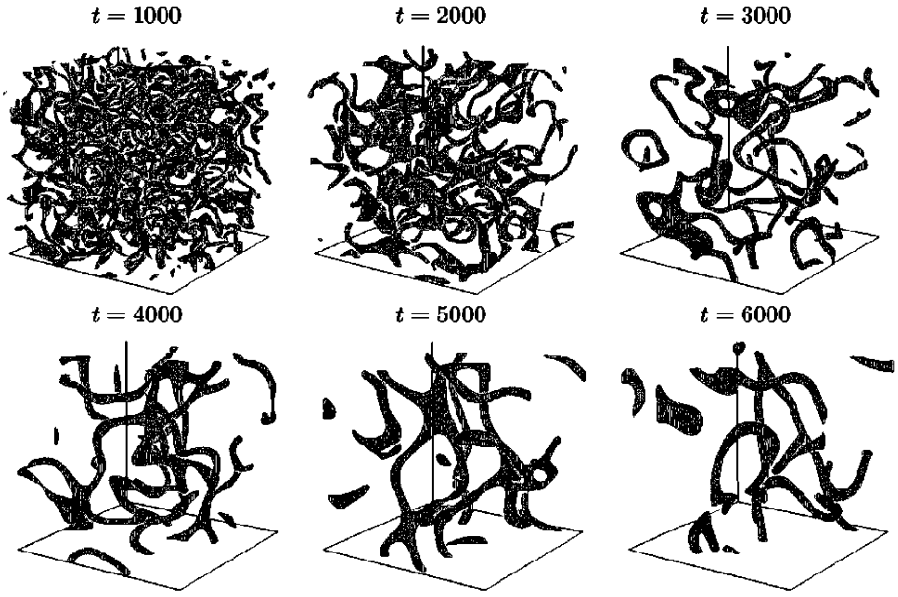

Fig. 1 Formation of superfluid turbulence in the process of strongly non-equilibrium kinetics of Bose-Einstein condensation governed by Gross-Pitaevskii equation, as simulated in Ref. [41]

The vortex lines reconnect producing the distortions (Kelvin waves), these distortions decay due to the drag force thereby reducing the total line length and rendering the tangle more and more dilute.

In contrast to the counter-flow setup, where the case $\alpha \ll 1$ can be considered rather specific, for the non-equilibrium process of Bose-Einstein condensation in a weakly interacting gas, the regime $\alpha \ll 1$ is quite characteristic in view of the following circumstance. The condensation kinetics is a classical-field process the essential part of which is quantitatively captured by the time dependent Gross-Pitaevskii equation (a.k.a. non-linear Schrödinger equation). Hence, the most natural setup is when the initial condition for the process features large occupation numbers for the bosons, and the whole process can be accurately described by the Gross-Pitaevskii equation from the very outset (see Fig. 1 for an illustration). In the idealized situation of the classical field, the final temperature asymptotically approaches zero in view of the ultraviolet catastrophe. Another situation where the regime $\alpha \ll 1$ occurs naturally is the quasi-classical turbulence, which, unlike counterflow turbulence, is due to a macroscopic turbulent motion and is generated by purely classical means at arbitrary temperatures without the help of mutual friction.

At $\alpha \ll 1$ ($\alpha \propto T^5$ at $T \to 0$, see Ref. [45]), dynamics of vortex lines in a significant range of length scales become essentially conservative. In this case, relaxation of turbulent motion in non-linear systems usually involves certain types of *cascades*. In both classical and superfluid turbulence the key role is played by the cascade of energy in the wavenumber space towards high wavenumbers. A realization of this peculiar relaxation regime is due to the following conditions satisfied by the system: (i) $\lambda_{\rm en} \gg \lambda_{\rm cutoff}$—a substantial separation of the energy-containing scale $\lambda_{\rm en}$ from the

scale $\lambda_{\rm cutoff}$ where the dissipation becomes appreciable, which defines the cascade *inertial range* $\lambda_{\rm en} > \lambda > \lambda_{\rm cutoff}$, (ii) the kinetics are local in the wavenumber space, i.e. the energy exchange is mainly between adjacent length scales, and (iii) the "collisional" kinetic time $\tau_{\rm coll}(\lambda)$—the time between elementary events of energy exchange at a certain scale λ—gets progressively shorter down the scales. These requirements determine the main qualitative features of the cascade: The decay is governed by the slowest kinetics at $\lambda_{\rm en}$, where the energy flux ε in the wavenumber space is formed, while the faster kinetic processes at shorter scales are able to instantly adjust to this flux supporting the transfer of energy towards $\lambda_{\rm cutoff}$, where it is dissipated into heat. Thus, the cascade is a (quasi-)steady-state regime in which the energy flux ε is constant through the length scales and the variation of ε in time happens on the longest time scale $\sim\tau_{\rm coll}(\lambda_{\rm en})$.

With vortex lines, one can think of quite a number of different cascades. Perhaps the most obvious one is the Richardson-Kolmogorov cascade of eddies, which can be realized in a superfluid (even at $T = 0$) due to its ability to emulate the classical-fluid turbulent motion by the motion of a polarized vortex-line tangle. Clearly, this type of the cascade is fundamentally impossible in the non-structured Kibble-Zurek-type tangle. For quite a long time it was believed that non-structured ST decays at $T = 0$ through the Feynman's cascade of vortex rings [46]. Feynman conjectured that reconnections of the vortex lines produce vortex rings, with subsequent decay of each ring into a pair of smaller rings, and so forth. It can be shown, however, that this conjecture is inconsistent with simultaneous conservation of energy and momentum for the daughter rings as soon as the coupling between separate rings becomes negligible (see Ref. [5] and Sect. 4), which necessarily happens below the length scale of interline separation. Another obvious option is a cascade of Kelvin waves supported by non-linear interaction (scattering) of kelvons. While such a cascade is indeed possible (see Ref. [13] and Sect. 3), it is subject to a peculiar constraint on the maximal energy flux. The origin of this constraint is the approximate integrability of the vortex dynamics controlled by the large parameter

$$\Lambda = \ln(\lambda/a_0), \tag{1}$$

where λ is the characteristic kelvon wavelength and a_0 is the vortex core radius. If the parameter Λ is large, then the leading term of the Kelvin-wave dynamics is given by the so-called local induction approximation (LIA) in which the velocity of an element of the vortex line is due to local differential properties of the line. The LIA dynamics turns out to be integrable, so that mere non-linearity of the LIA equations of motion does not lead to the Kelvin-wave cascade. This circumstance predetermines the existence of intermediate cascades that are necessary to transfer the energy to the wavenumbers high enough for the pure Kelvin-wave cascade to take over. All the intermediate cascades have to involve reconnections, to lift the constraint imposed by the integrability of LIA. In the non-structured tangle, there is only one type of reconnection-induced cascade. An elementary step of this cascade at the wavelength λ consists of two adjacent events: (i) emission of a vortex ring with the radius $\sim\lambda$ by a local self-crossing of a kinky vortex line and (ii) re-absorption of the ring by the tangle. Both events are accompanied by transferring Kelvin-wave energy to shorter wavelengths (but still on the order of λ), since reconnections of the vortex loops

produce Kelvin-wave structure with wavelength smaller than the loop radii. For the self-reconnection cascade to be efficient, the vortex line has to be kinky (loosely speaking, fractalized) at all relevant length scales. Due to the integrability of LIA, the fractalization is provided by the cascade itself: In the absence of self-crossings at a given length scale, the amplitude of Kelvin waves keeps growing due to self-crossings at larger length scales. It is worth emphasizing that in contrast to Feynman's scenario, where the vortex rings are the energy carriers, in the local self-crossing scenario, the rings play only a supportive role. In the process (i) a ring is just a product of self-crossing and in the process (ii) the ring is just a cause of yet another reconnection event. Clearly, the crucial part is played by Kelvin waves, which carry the energy, and reconnections, which directly promote the Kelvin-wave cascade.

In the polarized tangle emulating the Richardson-Kolmogorov classical-fluid cascade, there are two more varieties of reconnection-supported Kelvin-wave cascades. One is when reconnections are between the bundles of quasi-parallel vortex lines, and the other one when the reconnections are between two neighboring lines in a bundle. In Sect. 5 we present the arguments [20] that in the theoretical limit of $\Lambda \to \infty$, all the three reconnection driven cascades are necessary to cross over from Richardson-Kolmogorov to pure Kelvin-wave regime, the crossover being a series of three distinct cascades: bundle driven, neighboring reconnection driven, and local self-crossing driven. The total extent of the crossover regime in the Kelvin wavenumber space is predicted to be $\sim\Lambda/10$ decades. With realistic $\Lambda \lesssim 15$ (for ^{4}He), this means that the crossover takes about one decade, within which one can hardly expect sharp distinctions between the three different regimes.

At $T = 0$, the reconnection-supported cascade(s) ultimately crosses over to the pure Kelvin-wave cascade, and the latter is cut off by phonon emission [8, 10, 15]. The elementary process of phonon emission converts two kelvons with almost opposite momenta into one bulk phonon [15].

The rest of the paper is organized as follows. In Sect. 2 we render basic equations and notions of vortex dynamics: Biot-Savart equation and the LIA, Hasimoto representation for the LIA in terms of curvature and torsion, conservation of energy and momentum, Hamiltonian formalism for the Kelvin waves, conservation of angular momentum, implying conservation of the total number of kelvons. We pay special attention to the problem of *ultraviolet regularization* of the theory, crucial for an adequate treatment of non-local corrections to the LIA. In Sect. 3 we develop a theory of the pure Kelvin-wave cascade (supported by elastic scattering of three kelvons—the leading non-trivial scattering event consistent with conservation of energy, momentum, and the total number of kelvons). We show that the leading term in the three-kelvon scattering amplitude does not contain local contributions, in accordance with the integrability of LIA. We then find the spectrum and energy flux of the pure cascade. In Sect. 4 we analyze the scenario of local self-crossings, starting with the explanation why pure Feynman's cascade cannot be realized in view of conservation of momentum and energy. We show that this scenario implies fractalization of the vortex lines, and derive corresponding spectrum of Kelvin waves. We then discuss a simple Hamiltonian model [5] featuring a collapse-driven cascade in otherwise integrable system, and argue why the spectrum of the cascade in this model is similar to the one in the scenario of local self-crossings. In Sect. 5 we

address the problem of the crossover from Richardson-Kolmogorov to Kelvin-wave cascade. Section 6 is devoted to the theory of kelvon-phonon interaction. Starting from the hydrodynamical Lagrangian, we derive the Hamiltonian of kelvon-phonon interaction. The Hamiltonian allows us to straightforwardly formulate kinetics of the kelvon-phonon processes, and, in particular, find the cutoff momentum for the pure Kelvin-wave cascade. In Sect. 7 we summarize the main qualitative aspects of the theory and put our findings in the context of experiment and simulations, including the ones that are still missing. We also formulate certain theoretical questions to be addressed in the future. Finally, we critically discuss the concept of bottleneck between Richardson-Kolmogorov and Kelvin-wave cascades, put forward recently in Ref. [19] (see also Ref. [21]), which we disagree with on the basis of our theoretical analysis.

2 Basic Relations

2.1 Biot-Savart Law. Energy and Momentum

The zero-temperature hydrodynamics of a superfluid is nothing but the hydrodynamics of a classical ideal fluid with quantized vorticity—the only possible rotational motion is in the form of vortex filaments with a fixed value of velocity circulation κ. Therefore, one can apply the Kelvin-Helmholtz theorem of classical hydrodynamics—stating that the vortices move with the local fluid velocity—to obtain a closed dynamic equation for vortex filaments in a superfluid. Alternatively, one can start with the hydrodynamic action for the complex-valued field and derive the equation of vortex motion from the least-action principle. In the present section, we use the former approach, readily yielding the answer. (The latter approach will be used in Sect. 6.1, where it will prove crucial for describing the vortex-phonon interaction.)

If the vortex lines are the only degrees of freedom excited in the fluid, and if the typical curvature radius and interline separations are much larger than the vortex core size, a_0, then the instant velocity field at distances much larger than a_0 from the vortex lines is defined by the form of the vortex line configuration. Indeed, away from the vortex core the density is practically constant and the hydrodynamic continuity equation reduces to

$$\nabla \cdot \mathbf{v} = 0. \tag{2}$$

Then, taking into account that $\nabla \times \mathbf{v} = 0$ everywhere except for the vortex lines, and that for any (positively oriented) contour Γ surrounding one vortex line

$$\oint_{\Gamma} \mathbf{v} \cdot d\mathbf{l} = \kappa, \tag{3}$$

we note a direct analogy of our problem with the magnetostatic problem of finding magnetic field produced by thin wires: Velocity field is identified with the magnetic

field, and the absolute value of the current of each wire is one and the same and is proportional to κ. The result is given by the Biot-Savart formula

$$\mathbf{v}(\mathbf{r}) = \frac{\kappa}{4\pi} \int \frac{d\mathbf{s} \times (\mathbf{r} - \mathbf{s})}{|\mathbf{r} - \mathbf{s}|^3}, \tag{4}$$

where radius-vector $\mathbf{s}$ runs along all the vortex filaments.

According to Kelvin-Helmholtz theorem, each piece of the vortex line should move with a velocity corresponding to the velocity of the *net* motion of small contour (of the size, say, of order a_0) surrounding this element. This fact is very important, since the velocity field (4) is singular at all points on the vortex line, and the Kelvin-Helmholtz theorem yields a simple regularization prescription: Take a small circular contour with the center of the circle at some vortex line point and the plane of the circle perpendicular to the vortex line (at the point of intersection), and average the velocity field around the contour—to eliminate rotational component of the contour motion.

As is clear from (4), the singularity of the velocity field at some point $\mathbf{s} = \mathbf{s}_0$ in the vortex line comes from the integration over the close vicinity of the point $\mathbf{s}_0$. To isolate the singularity, we expand the function $\mathbf{s}(\xi)$ around the point $\mathbf{s}_0 = \mathbf{s}(\xi_0)$:

$$\mathbf{s} = \mathbf{s}_0 + \mathbf{s}'_\xi \xi + \mathbf{s}''_{\xi\xi} \xi^2/2 + \cdots. \tag{5}$$

Here ξ is the parameter of the line. It is convenient to use the natural parameterization, that is to choose ξ to be the (algebraic) arc length measured from the point $\mathbf{s}_0$. Substituting this expansion into (4), we get

$$\mathbf{v}(\mathbf{r} \to \mathbf{s}_0) = \frac{\kappa}{8\pi} \mathbf{s}'_\xi \times \mathbf{s}''_{\xi\xi} \int_{-\xi_*}^{\xi_*} \frac{d\xi}{|\xi|} + \text{regular part}, \tag{6}$$

where ξ_* is some upper cutoff parameter on the order of the curvature radius at the point $\mathbf{s}_0$. The integral in the right-hand side is divergent at $\xi \to 0$. To regularize it we note (i) that, by its very origin, the expression (4) is meaningful only at $|\xi| > a_0$, and (ii) the part of the vortex line with $|\xi| \ll a_0$ does not give a significant contribution to the net velocity on the contour of the radius $\sim a_0$. Hence, with a logarithmic accuracy we can adopt the regularization $|\xi| > a_0$, that is

$$\int_{-\xi_*}^{\xi_*} \frac{d\xi}{|\xi|} \to 2\ln(\xi_*/a_0). \tag{7}$$

Moreover, by fine-tuning the value of a_0 in accordance with a model-specific behavior at the distances $\sim a_0$, the logarithmic accuracy of the regularization (7) can be improved to the accuracy $\sim a_0/\xi_*$. We discuss this option in detail in Sect. 2.4, and utilize in Sect. 3.

We thus arrive at the Biot-Savart equation of vortex line motion

$$\dot{\mathbf{s}} = \frac{\kappa}{4\pi} \int \frac{d\mathbf{s}_0 \times (\mathbf{s} - \mathbf{s}_0)}{|\mathbf{s} - \mathbf{s}_0|^3}, \tag{8}$$

with the integral regularized in accordance with (7).

Equation (8) has two constants of motion:

$$\mathcal{E} = \int \frac{d\mathbf{s} \cdot d\mathbf{s}_0}{|\mathbf{s} - \mathbf{s}_0|}, \tag{9}$$

$$\mathcal{P} = \int \mathbf{s} \times d\mathbf{s}, \tag{10}$$

which (up to dimensional factors) are nothing than the energy and momentum, respectively.

2.2 Local Induction Approximation (LIA)

In the absence of significant enhancement of non-local interactions by polarization of the vortex tangle, the regular part in (6) is smaller than the first term containing large logarithm. In such cases it is often—but not always (!), see the theory of the pure Kelvin-wave cascade—safe to neglect the second term in (6) and proceed within LIA:

$$\dot{\mathbf{s}} = \beta \mathbf{s}'_\xi \times \mathbf{s}''_{\xi\xi}, \tag{11}$$

where

$$\beta = \frac{\kappa}{4\pi} \ln(R/a_0), \tag{12}$$

with the typical curvature radius R treated as a constant. Recalling that the parameter ξ in (6) is the arc length, it is crucial that equation of motion (11) is consistent with this requirement. (Speaking generally, in the course of evolution ξ might deviate from the arc length.) The consistency is established by directly checking that (11) implies

$$\frac{d}{dt} \sqrt{d\mathbf{s} \cdot d\mathbf{s}} = 0. \tag{13}$$

From (13) it trivially follows—by integrating over ξ—that the total line length is conserved. The total line length in LIA plays the same role as the energy (9) in the genuine Biot-Savart equation. Indeed, from (9) it is seen that within the logarithmic accuracy $\mathcal{E}$ is proportional to β times line length. It is not difficult to also make sure that (11) conserves $\mathcal{P}$ (10).

The standard constants of motion—the energy (line length), momentum, and angular momentum—are not the only quantities conserved by (11). For example, the integral of the square of the curvature radius is also conserved [47]:

$$\frac{d}{dt} \int (\mathbf{s}''_{\xi\xi})^2 d\xi = 0. \tag{14}$$

In the next section we will see that the constant of motion (14) is just one of the *infinite* set of constants of motion implied by the integrability of LIA.

2.3 Hasimoto Representation. Integrability of LIA

Betchov [47] revealed certain interesting properties of LIA, e.g., (14), by re-writing (11) in terms of intrinsic variables of the vortex line: curvature, ζ, and torsion, τ. Hasimoto [48] further advanced these ideas by discovering that for the complex variable $\psi(\xi, t)$, such that

$$\zeta = |\psi|, \qquad \tau = \frac{\partial \Phi}{\partial \xi} \tag{15}$$

(Φ is the phase of ψ) the LIA equation (11) is equivalent to the non-linear Schrödinger equation (time is measured in units β^{-1})

$$i\frac{\partial \psi}{\partial t} = -\frac{\partial^2 \psi}{\partial \xi^2} - \frac{1}{2}|\psi|^2\psi. \tag{16}$$

The one-dimensional non-linear Schrödinger equation is known to be an integrable system featuring and infinite number of additive constants of motion, the explicit form of which is given by [49]

$$\begin{aligned} I_n &= \int_{-\infty}^{\infty} \varphi_n(\xi) d\xi, \\ \varphi_1 &= \frac{1}{4}|\psi|^2, \\ \varphi_{n+1} &= \psi \frac{d}{d\xi}(\varphi_n/\psi) + \sum_{n_1+n_2=n} \varphi_{n_1}\varphi_{n_2}. \end{aligned} \tag{17}$$

The integrability of LIA renders any non-trivial relaxation kinetics impossible, unless the reconnections are involved to break the conservation of I_n's.

2.4 Hamiltonian Formalism

Suppose a vortex line can be parametrized by its Cartesian coordinates x and y as single-valued functions of the third coordinate z. In this case, the Biot-Savart law can be cast into a Hamiltonian form, very convenient for our purposes. First, introduce a vector $\boldsymbol{\rho}(z,t) = (x(z,t), y(z,t))$. In contrast to the earlier-defined vector $\mathbf{s}(\xi, t)$ that follows the motion of the element of fluid containing the element of vortex line, the vector $\boldsymbol{\rho}(z_0, t)$ just defines the geometrical point of intersection of the vortex line with the plane $z = z_0$. With this distinction in mind, it is easy to relate the time derivatives of the two vectors:

$$\frac{\partial \boldsymbol{\rho}}{\partial t} = \frac{\partial \mathbf{s}}{\partial t} - \left(\hat{z} \cdot \frac{\partial \mathbf{s}}{\partial t}\right)\left(\hat{z} + \frac{\partial \boldsymbol{\rho}}{\partial z}\right). \tag{18}$$

Here $\hat{z}$ is the unit vector in the z-direction. Substituting for $\partial \mathbf{s}/\partial t$ the right-hand side of (8), expressing then $\mathbf{s}$ in terms of $\boldsymbol{\rho}$, and finally replacing $\boldsymbol{\rho}$ with a complex variable $w(z,t) = x(z,t) + iy(z,t)$, we arrive at the Hamiltonian equation of vortex line motion:

$$i\dot{w} = \frac{\delta H}{\delta w^*}, \tag{19}$$

$$H = (\kappa/4\pi)\int \frac{\left[1+\mathrm{Re}\, w'^{*}(z_1)w'(z_2)\right]dz_1 dz_2}{\sqrt{(z_1-z_2)^2+|w(z_1)-w(z_2)|^2}}. \tag{20}$$

The Hamiltonian (20) is singular at $z_1 \to z_2$ and thus needs to be regularized. To this end we introduce r_* such that

$$a_0 \ll r_* \ll \lambda, \tag{21}$$

and write

$$H = H_{\mathrm{loc}} + H_{\mathrm{n.l.}} + \mathcal{O}(r_*/\lambda), \tag{22}$$

$$H_{\mathrm{n.l.}} = (\kappa/4\pi)\int\limits_{|z_1-z_2|>r_*} \frac{[1+\mathrm{Re}\, w'^{*}(z_1)w'(z_2)]dz_1 dz_2}{\sqrt{(z_1-z_2)^2+|w(z_1)-w(z_2)|^2}}, \tag{23}$$

$$H_{\mathrm{loc}} = 2\beta\int dz\sqrt{1+|w'(z)|^2}, \tag{24}$$

$$\beta = (\kappa/2\pi)\ln(r_*/a_*). \tag{25}$$

Here the value of $a_* \sim a_0$ is specially tuned to eliminate a factor of order unity in the logarithm. The absence of such a factor in (25) should not be confused with a lack of control on first sub-logarithmic corrections. In view of the first inequality in (21), the Hamiltonian $H_{\mathrm{n.l.}}$ is of purely hydrodynamic nature, while the Hamiltonian H_{loc} takes care of *both* hydrodynamic and microscopic (and system specific) features at distances smaller that r_*. In view of the condition $\lambda \gg a_0$, implied by (21), the microscopic specifics of the system is completely absorbed by the proper value of a_*. Indeed, whatever is the physics at the distances of the order of the vortex core radius, the leading contribution from these distances to the energy of a smooth vortex line should be directly proportional to the line length; and this is precisely what is expressed by (24).

The freedom of choosing a particular value of r_* within the range (21) can be used to introduce the local induction approximation by requiring that

$$\ln(r_*/a_0) \gg \ln(\lambda/r_*). \tag{26}$$

In this case, the Hamiltonian (22), with

$$\beta = (\kappa/2\pi)\ln(\lambda/a_0) = \Lambda\kappa/2\pi, \tag{27}$$

captures the leading—as long as the interline interactions are not relevant—logarithmic contribution, compared to which the non-local Hamiltonian (23) can be omitted with logarithmic accuracy guaranteed by the parameter $\Lambda^{-1} \ll 1$.

Less obvious technical trick is to *formally* set

$$r_* = a_* \tag{28}$$

to *nullify* the Hamiltonian $H_{\rm loc}$. Doing so might seem to violate the range of applicability of the essentially hydrodynamic Hamiltonian $H_{\rm n.l.}$.[1] Nevertheless, it is readily seen by inspection that under the condition $\lambda \gg a_0$ the resulting theory is equivalent to the theory (22)–(25) up to negligibly small corrections of the order a_0/λ. The resulting Hamiltonian is

$$H_{\rm psd} = (\kappa/4\pi) \int\limits_{|z_1-z_2|>a_*} \frac{[1 + \mathrm{Re}\, w'^*(z_1)w'(z_2)]dz_1 dz_2}{\sqrt{(z_1-z_2)^2 + |w(z_1)-w(z_2)|^2}}. \tag{29}$$

In direct analogy with the pseudo-potential method in the scattering theory, it has a status of a *pseudo*-Hamiltonian in the sense that, being a convenient but rather inadequate model at the scales $\sim a_0$, it accurately accounts for the long-wave motion of the vortex lines (including all sub-leading corrections to LIA coming from the distances $\sim a_0$) by an appropriate choice of a_*. In the next subsection, we describe an explicit procedure of extracting the value of a_* from a model-specific dispersion relation of Kelvin waves.

2.5 Kelvons. Angular Momentum and the Number of Kelvons

Suppose the amplitude of Kelvin waves (KW) is small enough, so that the following condition is satisfied:

$$\alpha(z_1, z_2) = \frac{|w(z_1) - w(z_2)|}{|z_1 - z_2|} \ll 1. \tag{30}$$

Linearizing (29) up to the leading orders in the dimensionless function $\alpha(z_1, z_2)$, we obtain

$$H_0 = (\kappa/8\pi) \int\limits_{|z_1-z_2|>a_*} \frac{dz_1 dz_2}{|z_1 - z_2|}\big[2\,\mathrm{Re}\, w'^*(z_1)w'(z_2) - \alpha^2\big]. \tag{31}$$

The Hamiltonian H_0 describes the linear properties of KW. It is diagonalized by the Fourier transformation $w(z) = L^{-1/2}\sum_k w_k e^{ikz}$ (L is the system size, periodic boundary conditions are assumed):

$$H_0 = (\kappa/4\pi)\sum_k \omega_k w_k^* w_k, \tag{32}$$

yielding Kelvin's dispersion law

$$\omega_k = \frac{\kappa}{4\pi}\left[\ln\frac{1}{ka_*} + C_0 + \mathcal{O}\big((ka_*)^2\big)\right]k^2, \tag{33}$$

with

$$C_0 = 2\int_1^\infty \frac{dx}{x}\big[\cos x + (\cos x - 1)/x^2\big] + 2\int_0^1 \frac{dx}{x}\big[\cos x - 1/2 + (\cos x - 1)/x^2\big] \approx -2.077. \tag{34}$$

[1] The authors acknowledge a discussion of this concern with Jason Laurie and Sergey Nazarenko.

Generally speaking, the term $\mathcal{O}((ka_*)^2)$ should be omitted, since it goes beyond the universality range of the pseudo-Hamiltonian (29). In each particular microscopic model this term will be sensitive to the details of the physics at the length scale $\sim a_0$. [With logarithmic accuracy, the constant C_0 can be omitted as well, while the specific value of a_* can be replaced with just and order-of-magnitude estimate a_0.]

The practical utility of (33) with sub-logarithmic correction C_0 (34) for a given specific microscopic model—*different* from the pseudo-Hamiltonian (29)—is as follows. Equations (33)–(34) can be used to *calibrate* the value of a_*, and thus fix the pseudo-Hamiltonian, by separately solving for the KW spectrum in the given microscopic model and then casting the answer in the form (33)–(34). Likewise, for a realistic strongly-correlated system like ^{4}He the appropriate value of a_* in the pseudo-Hamiltonian (29) can be calibrated by an experimentally measured kelvon dispersion.

Although the problem of KW cascade generated by decaying superfluid turbulence is purely classical, it will be convenient to approach it quantum mechanically—by introducing KW quanta, kelvons. In accordance with the canonical quantization procedure, we understand w_k as the annihilation operator of the kelvon with momentum k and correspondingly treat $w(z)$ as a quantum field. The Hamiltonian functional (29) is *proportional* to the energy—with the coefficient $\kappa\rho/2$, where ρ is the mass density—but not *equal* to it. This means that if one prefers to work with genuine Quantum Mechanics rather than a fake one (for our purposes, the latter is also sufficient), using true kelvon annihilation operators, $\hat{a}_k$, field operator $\hat{w}$, and Hamiltonian, $\hat{H}$, he should take into account proper dimensional coefficients: $\hat{H} = (\kappa\rho/2)H$, $\hat{w}_k = \sqrt{2\hbar/\kappa\rho}\hat{a}_k$. By choosing the units $\hbar = \kappa = 1$, $\rho = 2$, we ignore these coefficients until the final answers are obtained.

In the quantum approach, there naturally arises the notion of the number of kelvons. This number is *conserved* in view of its global $U(1)$ symmetry of the Hamiltonian, $w \to e^{i\varphi}w$ reflecting the rotational symmetry of the problem. The rotational symmetry is also responsible for the conservation of the angular momentum component along the vortex line direction. Thus the number of kelvons is immediately related to the angular momentum component [50]: one kelvon carries a single (negative) quantum, $-\hbar$, of the angular momentum component along the vortex line relative to the macroscopic angular momentum of the rectilinear vortex line.

Another advantage of the quantum language in weak-turbulence problems, which we intensively employ in this paper, is that the collision term of the kinetic equation immediately follows from the Golden Rule for the corresponding elementary processes.

3 Pure Kelvin-Wave Cascade

3.1 Qualitative Analysis

In the problem of low-temperature ST decay at the length scales smaller than the typical interline separation, the pure Kelvin-wave cascade on individual vortex lines is perhaps the most natural decay scenario one can think of. Indeed, the non-linear

nature of Kelvin-wave dynamics should allow such a process in which the energy in the form of Kelvin waves is transferred from the long-wave energy-containing modes to the short wavelengths where the dissipation becomes efficient. Provided with a wide inertial range, one could also expect such a transfer of energy to be local in the wavenumber space, in which case the relaxation is likely to be due to a cascade.

A subtlety that is immediately clear is the complete absence of kinetics in the leading approximation, which stems from the aforementioned integrability of the LIA, (11). If it exists, the pure Kelvin-wave cascade must be entirely due to the non-local coupling between different vortex-line elements. Hence, being suppressed by the small parameter $\Lambda^{-1} \ll 1$ relative to the leading LIA dynamics, the pure KW cascade is an *a priori* weak phenomenon. This fact provides us with an important consistency check of the results: the leading contribution $\propto \Lambda$—determined by the effective microscopic cutoff parameter a_*, if one uses the pseudo-Hamiltonian (29)—must completely drop out of the effective kelvon scattering amplitude.

The success of the Kolmogorov-type argumentation makes it very tempting to use a dimensional analysis of the dynamical equations of motion to immediately extract, e.g., energy spectra. Such a simple approach for Kelvin-wave turbulence, however, is doomed to failure. The reason is that here the scale invariance dictates the kinetics to be controlled by a purely geometrical *dimensionless* parameter $\alpha_k = b_k k$, where b_k is the typical KW amplitude at the wavenumber k. Thus, the solution could be only obtained from the corresponding kinetic equation, which reveals the proper combination of α_k and k the kinetics are due to. Deriving and solving the kinetic equation will be our main goal in the this section.

Let us first determine the general structure of the collisional term. The key aspects that essentially fix this structure are (i) the conservation of the number of kelvons, discussed in Sect. 2, (ii) the dimensionality of the problem, and (iii) weakness of non-linearities. The first circumstance means that the kinetics are entirely due to kelvon *elastic* scattering since the elementary events of kelvon creation/annihilation are prohibited. In other words, the only allowed kinetic channel is energy-momentum exchange between kelvons. On the other hand, the energy-momentum conservation laws in one dimension make this exchange impossible in two-kelvon collisions: the process $(k_1, k_2) \to (k_3, k_4)$ is only allowed if either $(k_3 = k_1,\ k_4 = k_2)$, or $(k_3 = k_2,\ k_4 = k_1)$ which does not lead to any kinetics. Thus any non-trivial kinetics can be only due to collisions of three or more kelvons.

The third condition translates into the fact that the amplitudes of Kelvin waves b_k in the pure cascade are necessarily small compared to their wavelengths, $\alpha_k = b_k k \ll 1$, at least at sufficiently large k. This is the central feature of this regime, which is due to the following. The cascade solution with the largest possible amplitudes, $\alpha_k \approx 1$, corresponds to the regime driven by self-reconnections, as described in Sect. 4, the regime where the non-linear effects are negligible altogether. The weakness of the purely non-linear kinetics makes the amplitude at a scale k rise (due to the energy supplied from the larger length scales) until b_k is of order $1/k$ and the self-reconnection can happen causing the energy transfer to a smaller scale. If non-linear processes are appreciable, smaller amplitudes b_k are sufficient to sustain the energy flux. Thus, the pure cascade spectrum, which due to the scale invariance has a general power-law form $\alpha_k = b_k k \propto k^\beta$, must be constrained by $\beta \leq 0$. Apart

from the marginal $\beta = 0$, the latter requirement guarantees that a theory built on $\alpha_k \ll 1$ becomes asymptotically exact at hight wavenumbers. Correspondingly, self-reconnections, being exponentially dependant on α_k, necessarily cease in the purely non-linear cascade.

The smallness of the Kelvin-wave amplitudes in the particle language means that the many-kelvon collisions are rare events and we can confine ourselves to the leading three-kelvon processes in the kinetic term.

These simple considerations already substantially limit the freedom in writing the collision term. In fact, the only missing ingredient, which needs to be calculated, is the wavenumber dependence of the effective kelvon scattering vertex. Postponing the final issue of finding this dependence until the next section, let us analyze the kinetic equation in a general form. Written in terms of averaged over the statistical ensemble kelvon occupation numbers $n_k = \langle a_k^\dagger a_k \rangle$, the kinetic equation is given by

$$\dot{n}_1 = \frac{1}{(3-1)!3!} \sum_{k_2,\ldots,k_6} \left(W_{4,5,6}^{1,2,3} - W_{1,2,3}^{4,5,6} \right). \tag{35}$$

Here $W_{1,2,3}^{4,5,6}$ is the probability per unit time of the elementary three-kelvon scattering event $(k_1, k_2, k_3) \to (k_4, k_5, k_6)$, and the combinatorial factor compensates multiple counting of the same scattering event. The three-kelvon effective interaction Hamiltonian has the general form

$$H_{\text{int}} = \sum_{k_1,\ldots,k_6} \delta(\Delta k) \tilde{V}_{1,2,3}^{4,5,6} a_6^\dagger a_5^\dagger a_4^\dagger a_3 a_2 a_1, \tag{36}$$

where the effective vertex $\tilde{V}$ is symmetrized with respect to the corresponding momenta permutations, $\delta(k)$ is understood as the discrete $\delta_{k,0}$, and $\Delta k = k_1 + k_2 + k_3 - k_4 - k_5 - k_6$. The probabilities $W_{1,2,3}^{4,5,6}$ are then straightforwardly given by the Fermi Golden Rule applied to the Hamiltonian (36):

$$\begin{aligned} W_{1,2,3}^{4,5,6} &= 2\pi |(3!)^2 \tilde{V}_{1,2,3}^{4,5,6}|^2 f_{1,2,3}^{4,5,6} \delta(\Delta\omega)\delta(\Delta k), \\ f_{1,2,3}^{4,5,6} &= n_1 n_2 n_3 (n_4 + 1)(n_5 + 1)(n_6 + 1), \\ \Delta\omega &= \omega_1 + \omega_2 + \omega_3 - \omega_4 - \omega_5 - \omega_6. \end{aligned} \tag{37}$$

Here the combinatorial factor $(3!)^2$ accounts for the addition of equivalent amplitudes. We are of course interested in the classical-field limit of (37), which is obtained by taking $n_k \gg 1$ and retaining only the leading in n_k terms. This procedure finally yields

$$\begin{aligned} \dot{n}_1 &= 216\pi \sum_{k_2,\ldots,k_6} |\tilde{V}_{1,2,3}^{4,5,6}|^2 \delta(\Delta\omega)\delta(\Delta k) \left(\tilde{f}_{4,5,6}^{1,2,3} - \tilde{f}_{1,2,3}^{4,5,6} \right), \\ \tilde{f}_{1,2,3}^{4,5,6} &= n_1 n_2 n_3 (n_4 n_5 + n_4 n_6 + n_5 n_6). \end{aligned} \tag{38}$$

The kinetic equation (38) supports an energy cascade [49], provided two conditions are met: (i) the kinetic time is getting progressively smaller (vanishes) in the

limit of large wavenumbers, (ii) the collision term is local in the wavenumber space, that is the relevant scattering events are only those where all the kelvon momenta are of the same order of magnitude. In the following subsection, we make sure that both conditions are satisfied: the condition (i) can be checked by a dimensional estimate, provided (ii) is true. The condition (ii) is verified numerically. Under these conditions one can establish the cascade spectrum by a simple dimensional analysis of the kinetic equation.

The locality of the collision term implies that the integral in (38) builds up around $(k_2, \ldots, k_6) \sim k_1$, which dramatically simplifies the kinetic equation:

$$\dot{n}_k \propto k^5 \cdot |\tilde{V}|^2 \cdot \omega_k^{-1} \cdot k^{-1} \cdot n_k^5, \tag{39}$$

where the factors go in the order of the appearance of corresponding terms in (38). At $k_1 \sim \cdots \sim k_6 \sim k$ we have $|V| \propto k^\nu$ and

$$\dot{n}_k \propto \omega_k^{-1} n_k^5 k^{4+2\nu}. \tag{40}$$

The energy flux (per unit vortex line length), θ_k, at the momentum scale k is defined as

$$\theta_k = L^{-1} \sum_{k' < k} \omega_{k'} \dot{n}_{k'}, \tag{41}$$

implying the estimate $\theta_k \sim k \dot{n}_k \omega_k$. Combined with (40), this yields $\theta_k \sim n_k^5 k^{5+2\nu}$, and the cascade requirement that θ_k be actually k-independent leads to the spectrum

$$n_k \propto \langle \hat{w}_k^\dagger \hat{w}_k \rangle = A k^{-(5+2\nu)/5}. \tag{42}$$

The value of the spectrum amplitude A in (42) controls the energy flux that the cascade transports. The relation between θ and A is

$$\theta = C_\theta \kappa^3 \rho A^5. \tag{43}$$

The dimensionless coefficient C_θ in this formula can be obtained, e.g., by a straightforward numerical calculation, as it was done by the authors in Ref. [13]. However, the calculation of Ref. [13] in view of a large relative error allowed to obtain only the order of magnitude of C_θ, which, as we explain in the next subsection, can be further questioned due to an erroneous omission of an order-one term in the effective vertex.

3.2 Quantitative Analysis

The central problem of this section is the derivation of the effective vertex $V_{1,2,3}^{4,5,6}$, which defines the effective kelvon interaction Hamiltonian (36) ($\tilde{V}$ is obtained from V by symmetrization with respect to corresponding momenta permutations). We start with the pseudo-Hamiltonian (29). Our fundamental requirement that the amplitude of KW turbulence is small as compared to the wavelength, $\alpha_k \ll 1$, is formulated by (30). This allows us to expand (29) in powers of $\alpha(z_1, z_2) \ll 1$: $H = E_0 + H_0 + H_1 + H_2 + \cdots$ (E_0 is just a number and will be ignored). The term H_0 is given by (31).

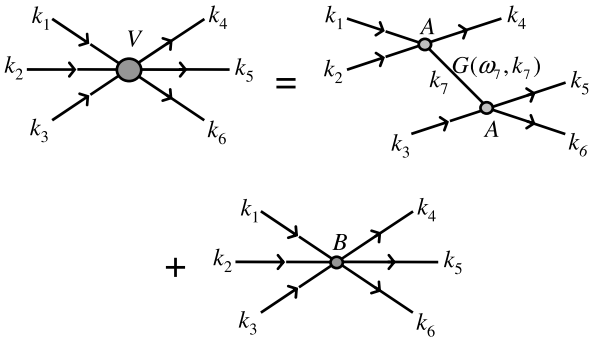

Fig. 2 The effective vertex of the three-kelvon scattering. The vertices A and B come from the terms H_1 (44) and H_2 (45) and are given by (46) and (47) respectively. $G(\omega, k)$ is the free kelvon propagator

As we demonstrated in the previous subsection, it describes the linear properties of the Kelvin waves, in particular it determines the Kelvin-wave dispersion law, (33). The higher-order terms are responsible for interactions between kelvons. The terms that will prove relevant are

$$H_1 = \frac{\kappa}{32\pi} \int\limits_{|z_1 - z_2| > a_*} \frac{dz_1 dz_2}{|z_1 - z_2|} [3\alpha^4 - 4\alpha^2 \operatorname{Re} w'^*(z_1) w'(z_2)], \tag{44}$$

and

$$H_2 = \frac{\kappa}{64\pi} \int\limits_{|z_1 - z_2| > a_*} \frac{dz_1 dz_2}{|z_1 - z_2|} [6\alpha^4 \operatorname{Re} w'^*(z_1) w'(z_2) - 5\alpha^6]. \tag{45}$$

As already demonstrated, the leading elementary process in our case is the three-kelvon scattering and the processes involving four and more kelvons are much weaker due to the inequality (30). The effective vertex, $V^{4,5,6}_{1,2,3}$, for the three-kelvon scattering [subscripts (superscripts) stand for the initial (final) momenta] consists of two different parts. The first part is due to the terms generated by the two-kelvon vertex, A (corresponding to the Hamiltonian H_1) in the second order of perturbation theory. [All these terms are similar to each other; we explicitly specify just one of them: $A^{4,7}_{1,2} G(\omega_7, k_7) A^{5,6}_{7,3}$. Here $G(\omega, k) = 1/(\omega - \omega_k)$ is the free-kelvon propagator, $\omega_7 = \omega_1 + \omega_2 - \omega_4$, $k_7 = k_1 + k_2 - k_4$.] The second part of the vertex V is the bare three-kelvon vertex, B, associated with the Hamiltonian H_2. The expression for the effective vertex is depicted diagrammatically in Fig. 2.

The explicit expressions for the bare vertices directly follow from (44) and (45) after the Fourier transform $w(z) = L^{-1/2} \sum_k w_k e^{ikz}$:

$$A = (6D - E)/8\pi, \tag{46}$$

$$D^{3,4}_{1,2} = \int_{a_*}^{L} (dx/x^5) \Big(1 - \big[{}_1\big] - \big[{}_2\big] - \big[{}^3\big] - \big[{}^4\big] + \big[{}^3_2\big] + \big[{}^{43}\big] + \big[{}^4_2\big]\Big),$$

$$
\begin{aligned}
E^{3,4}_{1,2} &= \int_{a_*}^{L} (dx/x^3)\Big\{k_4k_1\Big(\big[{}^{4}\big]+\big[{}_{1}\big]-\big[{}^{43}\big]-\big[{}^{4}_{2}\big]\Big)\\
&\quad + k_3k_1\Big(\big[{}^{3}\big]+\big[{}_{1}\big]-\big[{}^{43}\big]-\big[{}^{3}_{2}\big]\Big)+k_3k_2\Big(\big[{}^{3}\big]+\big[{}_{2}\big]-\big[{}^{43}\big]-\big[{}^{3}_{1}\big]\Big)\\
&\quad + k_4k_2\Big(\big[{}^{4}\big]+\big[{}_{2}\big]-\big[{}^{43}\big]-\big[{}^{3}_{2}\big]\Big)\Big\},\\
B &= (3P-5Q)/4\pi, \qquad (47)\\
P^{4,5,6}_{1,2,3} &= \int_{a_*}^{L}(dx/x^5)k_6k_2\Big\{\big[{}_{2}\big]-\big[{}^{5}_{2}\big]-\big[{}_{23}\big]+\big[{}^{5}_{23}\big]\\
&\quad -\big[{}^{4}_{2}\big]+\big[{}^{45}_{2}\big]+\big[{}^{4}_{23}\big]-\big[{}^{6}_{1}\big]+\big[{}^{6}\big]-\big[{}^{56}\big]\\
&\quad -\big[{}^{6}_{3}\big]+\big[{}^{56}_{3}\big]-\big[{}^{46}\big]+\big[{}^{456}\big]+\big[{}^{46}_{3}\big]-\big[{}_{12}\big]\Big\},\\
Q^{4,5,6}_{1,2,3} &= \int_{a_*}^{L}(dx/x^7)\Big\{1-\big[{}^{4}\big]-\big[{}_{1}\big]+\big[{}^{4}_{1}\big]-\big[{}^{6}\big]+\big[{}^{46}\big]\\
&\quad +\big[{}^{6}_{1}\big]-\big[{}^{46}_{1}\big]-\big[{}^{5}\big]+\big[{}^{45}\big]+\big[{}^{5}_{1}\big]-\big[{}^{45}_{1}\big]+\big[{}^{65}\big]-\big[{}^{456}\big]\\
&\quad -\big[{}^{56}_{1}\big]+\big[{}_{23}\big]-\big[{}_{3}\big]+\big[{}^{4}_{3}\big]+\big[{}_{13}\big]-\big[{}^{4}_{13}\big]+\big[{}^{6}_{3}\big]-\big[{}^{46}_{3}\big]-\big[{}^{6}_{13}\big]\\
&\quad +\big[{}^{5}_{2}\big]+\big[{}^{5}_{3}\big]-\big[{}^{45}_{3}\big]-\big[{}^{5}_{13}\big]+\big[{}^{6}_{2}\big]-\big[{}^{65}_{3}\big]+\big[{}_{12}\big]+\big[{}^{4}_{2}\big]-\big[{}_{2}\big]\Big\}.
\end{aligned}
$$

Here $\big[{}^{\cdots}_{\cdots}\big]$'s denote similar looking cosine functions, $\big[{}_{1}\big]=\cos k_1x$, $\big[{}^{4}_{1}\big]=\cos(k_4-k_1)x$, $\big[{}^{45}_{1}\big]=\cos(k_4+k_5-k_1)x$, $\big[{}^{45}_{12}\big]=\cos(k_4+k_5-k_1-k_2)x$, and so forth.

Since the microscopic physics at the scales $\sim a_0$ is quite complicated and usually not known precisely in strongly correlated systems like ^{4}He, it is important to asses the systematic error of the theory in the case when a_* can not be determined accurately. For this purpose, as well as for the convenience of the numerical analysis described below, we process the integrals (46), (47) as follows. We introduce a characteristic wavelength $\lambda\equiv\lambda(k_1,k_2,k_3,k_4,k_5,k_6)$, the particular functional form being not important. Then, from each of the integrals (46), (47), we subtract the corresponding LIA contributions, which are easily obtained by the same procedure that led to (46), (47) from the local Hamiltonian (24) defined by

$$\beta_\lambda=(\kappa/2\pi)\Lambda_\lambda,\qquad \Lambda_\lambda=\ln(\lambda/a_*). \tag{48}$$

As a result of the subtraction, up to system-specific terms $\sim(a_*/\lambda)^2$ to be neglected below, we get a_*-independent convergent integrals. Thereby we arrive at a convenient decomposition: $A=\Lambda_\lambda A^{(0)}+A^{(1)}$, $B=\Lambda_\lambda B^{(0)}+B^{(1)}$, where $A^{(0)}$ and $B^{(0)}$ are known analytically from LIA, while $A^{(1)}$ and $B^{(1)}$ are easily calculated numerically (see below for some useful details). On the technical side, the decomposition solves the problem of handling the logarithmic divergency, whereas physically, it clarifies the form of the dependence on the vortex-core details, which turn out to be entirely enclosed by LIA.

To proceed with estimating possible systematic errors, we introduce the expansion of the propagator G in the powers of inverse Λ_λ:

$$G = \Lambda_\lambda^{-1}[G^{(0)} + \Lambda_\lambda^{-1} G^{(1)} + \Lambda_\lambda^{-2} G^{(2)} + \mathcal{O}(\Lambda_\lambda^{-3})]. \tag{49}$$

For the vertex $V = AGA + B$ (see Fig. 2), we thus have

$$V = \Lambda_\lambda V^{(0)} + V^{(1)} + V^{(2)}/\Lambda_\lambda + \mathcal{O}(\Lambda_\lambda^{-2}), \tag{50}$$

with

$$\begin{aligned} V^{(0)} &= A^{(0)} G^{(0)} A^{(0)} + B^{(0)}, \\ V^{(1)} &= 2A^{(0)} G^{(0)} A^{(1)} + A^{(0)} G^{(1)} A^{(0)} + B^{(1)}, \\ V^{(2)} &= A^{(0)} G^{(2)} A^{(0)} + 2A^{(0)} G^{(1)} A^{(1)} + A^{(1)} G^{(0)} A^{(1)}. \end{aligned}$$

Note that by construction all the quantities $A^{(i)}$, $B^{(i)}$, $G^{(i)}$, and $V^{(i)}$ are a_*-independent, since the dependence on a_*—up to the neglected terms $\sim(a_*/\lambda)^2$—comes exclusively through Λ_λ. The term $\Lambda_\lambda V^{(0)}$ is precisely the effective vertex that follows from the LIA Hamiltonian (24), and thus it necessarily obeys $V^{(0)} \equiv 0$. The leading contribution to V is the a_*-independent $V^{(1)}$. Thus, the short-range physics enters the answer only as a small in $1/\Lambda_\lambda$ correction.

Now we are in a position to specify the systematic error due to uncertainties in microscopic details. In the case when it is possible to calibrate the pseudo-Hamiltonian, that is to find (analytically or experimentally, see Sect. 2) the accurate value of a_*, the systematic error is of order $(a_*/\lambda)^2$. Otherwise, we are forced to set $a_* \sim a_0$, meaning that the parameter $\Lambda_\lambda \gg 1$ is only known up to $\delta\Lambda_\lambda \sim 1$, which for the systematic uncertainty in V gives $V^{(2)}\delta\Lambda_\lambda/\Lambda_\lambda^2 \sim 1/\Lambda_\lambda^2$. We thus arrive at an important conclusion that even if the microscopic details, such as the vortex-core shape, are completely unknown, by naively setting $\Lambda_\lambda = \ln(\lambda/a_0)$ we are paying by a relative error of only $1/\Lambda_\lambda^2$.

A comment is in order here on the technical issue of a convenient handling of the integrals, which we do numerically, upon subtracting the logarithmic singularity. The whole procedure is almost identical to the one that led us to the kelvon dispersion, (33)–(34). The new aspect is the dependence on four/six momenta, rendering a direct tabulation of integrals computationally expensive. The trick is to split a four/six-parametric integral into a sum of single-parametric integrals. A minor technical problem comes from the power-law divergence at $x \to 0$ of each separate single-parametric integral in (46), (47). The problem is readily solved by introducing power-law counter-terms—the *net* contribution of which is identically equal to zero—rendering each individual single-parametric integral convergent. As an illustration, we present the final result for the regularized (by subtracting the LIA terms and introducing the counter-terms) integral D of (46), which we denote with $\tilde{D}$. With the re-scaled (by $x \to \lambda x$) integration variable, the expression reads

$$\begin{aligned} \tilde{D}^{3,4}_{1,2} = \lambda^{-4} \int_1^\infty (dx/x^5) \Big(1 - \big[{}_1\big] - \big[{}_2\big] - \big[{}^3\big] - \big[{}^4\big] + \big[{}^3_2\big] + \big[{}^{43}\big] + \big[{}^4_2\big] \Big) \\ + \lambda^{-4} \int_0^1 (dx/x^5) \Big(\big[\!\big[{}^3_2\big]\!\big] + \big[\!\big[{}^{43}\big]\!\big] + \big[\!\big[{}^4_2\big]\!\big] - \big[\!\big[{}_1\big]\!\big] - \big[\!\big[{}_2\big]\!\big] - \big[\!\big[{}^3\big]\!\big] - \big[\!\big[{}^4\big]\!\big] \Big). \end{aligned} \tag{51}$$

Here $\left[\begin{smallmatrix}\cdots\\ \cdots\end{smallmatrix}\right]$'s denote the same cosines as previously, but with an extra factor λ in the argument due to re-scaled x. The symbol $\left[\!\left[\begin{smallmatrix}\cdots\\ \cdots\end{smallmatrix}\right]\!\right]$ means that for the cosine, we subtract first few—first three in the case of $\tilde{D}$—terms of its Taylor expansion to render corresponding single-parametric integral convergent (and thus individually tabulatable).

Note that recently closed analytic expressions for the vertex integrals (46), (47) were obtained in Ref. [28]. The authors of Ref. [28] followed a similar approach of handling the singularity as described above, but went further and solved the remaining convergent integrals.

From (46), (47) it is straightforward to obtain the scaling of the effective vertex V with the momenta—at $k_1 \sim \cdots \sim k_6 \sim k$ we have $|V| \sim k^6$. Thus, $\nu = 6$ in (42) and the pure Kelvin-wave cascade spectrum (restoring all the dimensional coefficients) is

$$\langle \hat{w}_k^\dagger \hat{w}_k \rangle = \frac{2\hbar n_k}{\kappa\rho} = Ak^{-17/5}. \tag{52}$$

This result was corroborated in a direct numerical simulation by the authors [14], where the spectrum (52) was resolved with a high accuracy allowing us to distinguish it from $n \propto k^{-3}$ suggested in an earlier simulation by Vinen et al. [12]. The high precision required to distinguish the close exponents, both in terms of the cascade inertial range extent and low noise, was achieved using a special numerical scheme developed to reduce the complexity of the non-local model (29) to that of an effectively local one at an expense of a controllable systematic error. We refer to Ref. [13] for more details.

Let us also express the spectrum in terms of the typical geometrical amplitude, b_k, of the KW turbulence at the wavevector $\sim k$. By the definition of the field $\hat{w}(z)$ we have: $b_k^2 \sim L^{-1} \sum_{q\sim k} \langle \hat{w}_k^\dagger \hat{w}_k \rangle \sim k \langle \hat{w}_k^\dagger \hat{w}_k \rangle$. Hence, using (43), we obtain

$$b_k \sim (\Theta/\kappa^3\rho)^{1/10} k^{-6/5}. \tag{53}$$

One can convert (52) into the curvature spectrum. For the curvature $\mathbf{c}(\zeta) = \partial^2\mathbf{s}/\partial\zeta^2$ [where $\mathbf{s}(\zeta)$ is the radius-vector of the curve as a function of the arc length ζ], the spectrum is defined as Fourier decomposition of the integral $I_c = \int |\mathbf{c}(\zeta)|^2 \, d\zeta$. The smallness of α, (30), allows one to write $I_c \approx \int dz \langle \hat{w}''^\dagger(z) \hat{w}''(z) \rangle = \sum_k k^4 n_k \propto \sum_k k^{3/5}$, arriving thus at the exponent 3/5.

So far we were heavily relying on the assumption of locality of the kinetic processes in the wavenumber space. We checked [13] the validity of this assumption by a numerical analysis of the kinetic equation thereby (i) making sure that the collision term of the kinetic equation is local and (ii) estimating the value of the dimensionless coefficient in (43) (see, however, below). The analysis is based on the following idea [51]. Consider a power-law distribution of occupation numbers, $n_k = A/k^\beta$, with the exponent β arbitrarily close, but not equal, to the cascade exponent $\beta_0 = 17/5$. Substitute this distribution in the collision term of the kinetic equation—right-hand side of (38). Given the scale invariance of the power-law distribution, the following alternative takes place. Case (1): collision integral converges for β's close to β_0, and, in accordance with a straightforward dimensional analysis, is equal to

$$\mathrm{Coll}([n_k = A/k^\beta], k) = C(\beta) A^5 \omega_k^{-1} / k^{5\beta-16}. \tag{54}$$

Here $C(\beta)$ is a dimensionless function of β, such that $C(\beta_0) = 0$ since the cascade is a steady-state solution. Case (2): collision integral diverges for β close to β_0. The case (2) means that the collision term is non-local and the whole analysis in terms of the Kolmogorov-like cascade is irrelevant. Fortunately, our numerics show that we are dealing with the case (1). Substituting (54) for $\dot{n}_k$ in (41), we obtain the expression $\theta_k(\beta) = (A^5/2\pi)k^{17-5\beta}C(\beta)/(17-5\beta)$. Taking the limit $\beta \to \beta_0$, we arrive at the k-independent flux $\theta = -C'(\beta_0)A^5/10\pi$.

In Ref. [13], we used this formula to obtain the coefficient in (43) by calculating $C(\beta)$ and finding its derivative $C'(\beta_0) = -10\pi C_\theta$. We simulated the collision integral by Monte Carlo method. The integrals (46), (47), were calculated numerically. However, a mistake was made at the level of combining these integrals into the effective vertex V. Due to the cancellation of the leading logarithmic terms one has to keep an accurate account of the sub-logarithmic corrections, including those in the kelvon propagator $G(\omega, k) = 1/(\omega - \omega_k)$ as well, as we already demonstrated above. Unfortunately, we failed to appreciate a simple fact that the constant C_0 appearing in the kelvon dispersion (33) results in an order-one contribution to the effective vertex V, and neglected this constant in the propagator. Since the coefficient $C_\theta \approx 10^{-5}$ was obtained in Ref. [13] only as an order of magnitude estimate (with an error $\sim$75% due to a slowing down of the high-order numerical integration) the mistake might not significantly effect this result, but still makes it questionable. A more accurate determination of C_θ is necessary. The use of analytic expressions for the vertex integrals obtained in Ref. [28] should substantially simplify the calculation.

In the paper by Nemirovskii [26], a question was raised of whether the purely nonlinear kelvon cascade gets distorted or perhaps even becomes irrelevant in real tangles due to the presence of reconnections. Although in our model we did not explicitly account for the splitting and merging of the vortex lines that carry kelvons, the validity of doing so is guaranteed by the locality of the cascade in the wavenumber space, which implies that the processes at larger length scales, such as the reconnections discussed in detail in the following section, can not influence the nonlinear kinetics other than by providing the energy flux θ as an input parameter. As an explicit check, one can demonstrate that the kinetic times $\tau_{\rm coll}(\lambda) \propto \lambda^{2/5}$ corresponding to the pure cascade solution (52), (53) are getting progressively smaller than the typical time between reconnections, which is given by the kelvon turnover (dynamical) time $\tau_{\rm dyn}(\lambda_*)$ at the crossover scale λ_* between the reconnection-driven and the pure cascades (see Sect. 4.3).

4 Self-Reconnection Driven Cascade

4.1 Absence of Feynman's Cascade

For quite a long period of time it has been generally accepted that at $T = 0$ the scenario of decay of superfluid turbulence is the one proposed by Feynman [46]. Namely, that vortex lines first decay into vortex rings, each of the rings then independently self-reconnects, producing smaller rings, each of the smaller rings self-reconnects to produce even smaller rings, and so forth. In this respect it is very characteristic

that even after the absence of pure Feynman's cascade was directly shown, and the scenario of Kelvin-wave cascade driven by local self-crossings was proposed [5], simulations of the low-temperature decay within LIA performed in Ref. [9] were still interpreted in terms of Feynman's cascade.

The problem with Feynman's cascade is that it is inconsistent with simultaneous conservation of energy and momentum for the vortex rings in the quantized regime [5]. As long as coupling between separate vortex lines is appreciable relative to the self-induced motion described by the LIA (11), the Feynman's processes are allowed since, while the momentum of the tangle is given by it's spanned area (10), the energy (9) is stored in both the vortex-line length and the interline coupling. Once, however, the line coupling becomes negligible, as, e.g., near the scale of interline separation, making the energy and the momentum of the rings additive, the Feynman scenario must quickly cease. This is clear from the mere fact that in this case the energy scales as the length of the ring (up to logarithmic corrections) while the momentum scales as the length squared, so that a decay into arbitrarily small rings with the net line length conserved would result in vanishing total momentum. In disordered tangles, where the energy-containing scale is the scale of interline spacing, this means that the Feynman's scenario has no appreciable inertial range, although Feynman's processes can take place at larger scales [26] irrelevant for kinetics. In quasi-classical tangles, the Feynman's mechanism is a constituent of the complex non-linear dynamics in the Kolmogorov regime.

4.2 Generation of Kelvin Waves in the Process of Line Reconnection

With a slight modification of the time dependence of the phase, the standard self-similar solution of the linear Schrödinger's equation—its Green's function—applies also to the non-linear equation (16). Indeed, the absolute value of the solution is spatially homogeneous, so that the non-linearity is equivalent to a spatially homogeneous time dependent external potential that can be immediately absorbed into the phase as an extra time-dependent term. The result is

$$\psi(\xi, t) = \frac{A}{\sqrt{t}} \exp\left[i \left(\frac{\xi^2}{4t} + \frac{A^2}{2} \ln |t| \right) \right]. \tag{55}$$

In accordance with (15), this solution implies

$$\xi = A/\sqrt{t}, \tag{56}$$

$$\tau = \xi/2t. \tag{57}$$

The physical meaning of the solution (56)–(57), first revealed by Buttke [52], is the relaxation of the vortex angle, the value of which is controlled by the parameter A. This solution gives an accurate description (within LIA) of relaxation of two vortex lines after their reconnection, as long as the curvature in the relaxation region remains much larger than the curvatures of the two lines away from the region, so that the distant parts of the two lines can be approximately treated as straight lines. By dimensional argument, the self-similarity regime should be achieved very rapidly

upon the reconnection, with the velocity of propagation of the fastest Kelvin waves (with wave vectors $\sim a_0$).

With the solution (56)–(57) one can explicitly see that reconnections lift the integrability constraints. At $\xi \to \infty$ we have $\varphi_n \sim \xi^n$, meaning that a single reconnection renders all the integrals I_n (17) divergent.

Let us look at the asymptotic form of the solution (56)–(57) in Cartesian coordinates, taking the direction of the z-axis along one of the two lines, $z \to +\infty$ corresponding to the asymptotic limit:

$$x(z,t) + iy(z,t) = (4At^{3/2}/z^2)e^{iz^2/4t}, \quad z \gg \sqrt{t}. \tag{58}$$

Equation (58) reveals a helical Kelvin-wave structure moving away from the reconnection region. It is important that while arbitrarily small wavelengths are present in the solution (58), the integral for the total line lengths comes from the largest length scale $z \sim \sqrt{t}$. This provides a support for two crucial points of the scenario of self-reconnections driven Kelvin-wave cascade: (i) Reconnections push Kelvin waves to smaller lengthscales, (ii) apart from higher-order corrections, the line length associated with the curvature radius R cannot go directly to the scales of curvature radius much smaller than R (locality of the cascade in the wavenumber space).

When the angle between the two lines is close to π, the reconnection leads to a production of vortex rings [52]. This process does not introduce a new cascade channel. Qualitatively it is very similar to the pure production of Kelvin waves (58) because, up to higher-order corrections, the line length is being transferred to the rings of the radii of the order of the curvature radii of reconnecting lines, i.e. to adjacent scales in the kelvon wavenumber space.

Being violent events, reconnections of vortex lines generally speaking result in radiation of sound. However, since the emission is mainly from the singular vortex angle, the fraction of vortex length being directly converted into sound during a reconnection is negligibly small by the parameter a_0/R, as compared to the fraction of the vortex length being converted into kelvons.

4.3 Fractalization of Lines. Kelvin-Wave Spectrum

In this subsection we render the analysis of Ref. [5] of the fractalization of a vortex line by the self-crossings driven Kelvin-wave cascade. We start with introducing the crucial notion of a smoothed line length, $\mathcal{L}(\lambda_1)$, which is the length of a (fractalized) line upon smoothing out all the structures of the length scales smaller than λ_1. Corresponding mathematical expression reads

$$\ln \mathcal{L}(\lambda_1) \sim \ln \mathcal{L}(\lambda_0) + \int_{\lambda_1}^{\lambda_0} (b_\lambda/\lambda)^2 d\lambda/\lambda, \tag{59}$$

where b_λ, defined in Sect. 3.2, is the characteristic amplitude of the Kelvin-wave structure at the wavelength λ, while λ_0 is, generally speaking, *any* fixed wavelength scale significantly larger than λ_1. In particular, if λ_0 is the largest wavelength of the problem, then $\mathcal{L}(\lambda_0)$ is the length of maximally smoothed vortex line. With $\mathcal{L}(\lambda)$ we

can estimate the number of local self-crossings at the scale λ per unit time as

$$N_\lambda \sim \frac{\mathcal{L}(\lambda)}{\lambda}\Omega_{b_\lambda}(\lambda)\omega_\lambda, \tag{60}$$

where the factor $\mathcal{L}(\lambda)/\lambda$ gives the number of statistically independent pieces of the line (at the wavelength scale λ typical correlation length is $\sim\lambda$), the factor $\Omega_{b_\lambda}(\lambda)$ is the probability of the Kelvin-wave amplitude fluctuation given the spectrum b_λ within a line element of the length $\sim\lambda$, such that the amplitude is of order λ in order to produce a self-crossing, and ω_λ is the kelvon frequency playing the role of inverse correlation time.

To estimate $\Omega_{b_\lambda}(\lambda)$, we can rely on the theoretical limit of $b_\lambda \ll \lambda$, in which kelvons are independent harmonic modes and, correspondingly, the statistics of fluctuations of the amplitude is Gaussian. This readily yields

$$\Omega_{b_\lambda}(\lambda) \sim (b_\lambda/\lambda)\mathrm{e}^{-(\lambda/b_\lambda)^2}. \tag{61}$$

We do not introduce any dimensionless factor in the Gaussian exponent in view of the freedom of defining b_λ up to a factor of order unity.

For any cascade the fundamental notion is the flux of corresponding conserved quantity. In our case, it is the flux of the vortex line length. The fractalization of the lines introduces certain subtleties. In contrast to a standard cascade in which the integral for the conserved quantity comes from a single length scale, in our case the line length is spread over all scales of distance of the inertial range. Moreover, different wavelength scales are not *entirely* independent in the sense that with the fractalized lines the short-range structures with their energy are slaved by the long-wave structures. So that the line length coming from long waves to shorter ones is essentially carried by short-ranged structures slaved by the long-wave modes. The crucial observation now is that with respect to larger wavelengths the slaved shorter wavelengths play a rather passive role in energy balance, since short-wave contribution to line length carried by the longer waves is just proportional to the smoothed line length. Correspondingly, one can speak of the *smoothed* line length flux, $Q(\lambda_1)$, where λ_1 is the smoothing parameter of (59). By definition of the cascade, the quantity Q is one and the same for any wavelength scale λ, as long as $\lambda \gg \lambda_1$.

Having fixed some wavelength scale λ, we note that the self-reconnections scenario implies

$$Q(\lambda_1) \sim N_\lambda \mathcal{R}_\lambda(\lambda_1), \tag{62}$$

where $\mathcal{R}_\lambda(\lambda_1)$ is the length of a λ_1-smoothed circle of the radius $\sim\lambda$. In a direct analogy with (59), we have

$$\ln \mathcal{R}_\lambda(\lambda_1) \sim \ln\lambda + \int_{\lambda_1}^{\lambda} (b_{\lambda'}/\lambda')^2 d\lambda'/\lambda'. \tag{63}$$

From (63) and (59) the follows a useful relation

$$\mathcal{L}(\lambda)\mathcal{R}_\lambda(\lambda_1) \sim \lambda\mathcal{L}(\lambda_1). \tag{64}$$

With N_λ (60) , $\Omega(\lambda)$ (61), the estimate $\omega_\lambda \sim \beta/\lambda^2$, and the relation (64), (62) yields

$$Q(\lambda_1)/\mathcal{L}(\lambda_1) \sim (\beta b_\lambda/\lambda^3)\mathrm{e}^{-(\lambda/b_\lambda)^2}. \tag{65}$$

The left-hand side of this relation is a function of λ_1, while the right-hand side is a function of λ, meaning that both sides are actually constants. For the right-hand side this implies

$$(b_\lambda/\lambda)^2 \sim \frac{(b_{\lambda_0}/\lambda_0)^2}{1+(b_{\lambda_0}/\lambda_0)^2\ln(\lambda_0/\lambda)}. \tag{66}$$

(Since up to logarithmic corrections we have $b_\lambda \sim \lambda$, we do not distinguish between $\ln b_\lambda$ and $\ln\lambda$.) Expression (66) yields the Kelvin-wave cascade spectrum in terms of the characteristic amplitude b_λ. As far as the function $\mathcal{L}(\lambda)$ is concerned, from (66) and (59) we find

$$\mathcal{L}(\lambda) = \mathcal{L}(\lambda_0)\left[1+\left(\frac{b_{\lambda_0}}{\lambda_0}\right)^2\ln\frac{\lambda_0}{\lambda}\right]^\nu, \tag{67}$$

where ν is a constant of order unity the particular value of which cannot be established by our order-of-magnitude analysis.

It is clear from (53) that no matter how large the energy flux (per unit vortex-line length) $\theta \propto Q$ transported by the self-crossings regime is, at sufficiently high wavenumbers the pure Kelvin-wave cascade will be capable of supporting it. As soon as the purely non-linear kinetics become appreciable, the amplitudes of Kelvin waves must become smaller, which in view of (61), inhibits the reconnections. Thus, the self-crossings-driven regime will inevitably be replaced by the pure Kelvin-wave cascade at some scale λ_*. Note, however, that due to a small difference between the Kelvin-wave spectra in the two regimes, (53), (66), the crossover between them is likely to be extended in the wavenumber space. A rough estimate of the scale λ_* can be obtained by setting $b_k \sim k^{-1} \sim \lambda_*$ in (53). The result clearly depends on the cascade energy flux θ, which is specific to the physics at the energy-containing scale. In quasi-classical turbulence, θ is related to the Kolmogorov energy flux, in which case an estimate for λ_* will be obtained in Sect. 5. In the case of a non-structured tangle, the energy flux is formed by reconnections at the scale of interline separation l_0, $\theta_{\mathrm{ns}} \sim \kappa^3\rho\Lambda^2/l_0^2$, with $\Lambda = \ln(l_0/a_*)$, which gives

$$\lambda_* \sim l_0/\Lambda \quad \text{(non-structured tangles)}. \tag{68}$$

According to this rough estimate, the inertial range for the regime driven by local self-crossings is only about $\Lambda/10$ decades, which for realistic values of Λ could turn out to be an insignificant range without a distinct spectral signature. Thus, it would be crucial to quantify the crossover between the regimes by a direct numeric simulation.

4.4 Qualitative Hamiltonian Model

The Hamiltonian description (19) implies single-valuedness of the function $w(z)$. Amazingly, the question of what happens to the mathematical solution of (19) when the physical function $w(z)$ becomes non-single valued turns out to be very relevant

to the theory of self-crossings driven cascade. Clearly enough, the mathematical solution has to develop a certain singularity, and, strictly speaking, become ill defined afterwards. However, if one introduces a discretized analog of the problem described by the Hamiltonian [5] (we confine ourselves to LIA),

$$i\dot{w}_n = \frac{\partial H}{\partial w_n^*}, \quad H = \sum_{n=0}^{N-1} \sqrt{1 + |w_{n+1} - w_n|^2}, \tag{69}$$

the Hamiltonian dynamics remains well-defined at any time moment. Numerical analysis of this model [5] shown that the above-mentioned singularity evolves into a finite jump between the values of w_j and w_{j+1}, at a certain j. The jump exists for a certain time, and then relaxes, the relaxation process being qualitatively similar to the process of vortex angle evolution in the sense that Kelvin waves are being emitted, while the integrability constraint is naturally lifted by non-smoothness of the function. With the precise geometric meaning of the Hamiltonian (69)—the length of the broken line defined by the points $\{w_n\}$—we realize that the dynamics governed by it should be qualitatively equivalent to the self-reconnection induced cascade, leading to the fractalization of the line necessary to support jumps of arbitrarily small amplitude, the amplitude of the jump playing qualitatively the same role as the radius of the ring in the self-crossings driven cascade. And that is precisely what has been revealed by numeric simulation of the model (69) in Ref. [5]. The simulations also revealed the spectrum $b_\lambda \sim \lambda$, consistent with (66), the logarithmic factor going beyond numeric resolution.

5 Crossover from Richardson-Kolmogorov to Kelvin-Wave Cascade

5.1 Quasi-Classical Tangles at $T = 0$: Crossover to the Quantized Regime

Even at absolute zero temperature the superfluid dynamics supports a turbulent regime, which under certain conditions is indistinguishable from classical turbulence [4]. That may seem quite surprising since the only degrees of freedom in a superfluid at $T = 0$ are quantized vortex lines, which are singular topological objects and thus are very different from the classical eddies responsible for turbulence in classical ideal incompressible fluids. Nonetheless, quantized vortex lines possess a mechanism that allows them to mimic classical vorticity—it is well known [1] that macroscopic velocity profile of a rapidly rotated superfluid mimics solid-body rotation, which is accomplished by formation of a dense array of vortex lines aligned along the rotation axis. The basis of this mechanism is the strong coupling between the vortex lines in the dense array, which makes such a bundle behave as a single coherent classical object. Therefore, by essentially classical turbulence generation methods (i.e. "stirring") one can produce vorticity in the *course-grained* up to length scales larger than the typical interline separation l_0 superfluid velocity field, indistinguishable from that of a normal fluid, the underlying vortex tangle being organized in polarized "bundles" of vortex lines.

Over the last decade, experimental observations of the classical behavior exhibited by superfluids [16, 18, 23, 37–40] have largely led to a renaissance of general interest in superfluid turbulence. Perhaps the most attractive feature of this quasi-classical turbulence is that, unlike counterflow turbulence, it in principle allows generation and probing at temperatures close to absolute zero. (It is only very recently that a unique technique of non-structured tangle (à la counterflow turbulence) production at very low temperatures was developed by the Manchester group [23].) With recent technological advances this opens an intriguing possibility of studying such essentially low-temperature phenomena as, e.g., the Kelvin-wave cascades.

However, it was recently realized [19] that, at $T = 0$, the question of how the quasi-classical vortex tangle looks like when one zooms in down to scales of order l_0, where the vorticity is essentially discrete, is quite a puzzling problem. The only fact that is immediately clear is that near the scales $\lambda_{\rm ph} \ll l_0$ where the dissipation due to the sound radiation takes place, the energy flux must be transported by the pure Kelvin-wave cascade. What happens in the intermediate regime between the classical Kolmogorov cascade of eddies and the Kelvin-wave cascade on individual vortex lines is the subject of this section.

In their scenario, L'vov, Nazarenko, and Rudenko [19], noted that a simple picture in which the pure Kelvin-wave cascade supersedes the Kolmogorov regime at the scale l_0 is not possible. The difficulty is due to the fact that at this scale the pure Kelvin-wave cascade is unable to sustain the Kolmogorov energy flux (per unit mass of the fluid) ε. Correspondingly, L'vov, Nazarenko, and Rudenko put forward an idea of bottleneck accumulation of energy at the classical scales adjacent to l_0. The accumulation of energy in the form of a thermalized distribution of quasi-classical vorticity was suggested to be necessary to raise the level of turbulence to a value at which the pure Kelvin-wave cascade becomes efficient. Note, however, that the concept of bottleneck at a given scale fundamentally relies on the absence of *any* efficient energy transport mechanism at this scale. Due to this fact, under the conditions of Ref. [19], vortex-line reconnections play a fatal role for the bottleneck scenario. Indeed, if the Kolmogorov cascade can reach the scale l_0 as assumed in Ref. [19], the typical vortex-line curvature at this scale is of the order l_0 meaning that the vortex-line reconnections must happen due to the tangle geometry, which makes them an alternative energy transport channel to the pure Kelvin-wave cascade. Estimating the energy flux $\varepsilon_{\rm rec}$ processed by the reconnections at this scale we see that $\varepsilon_{\rm rec}/\varepsilon \sim \Lambda^2 \gg 1$, i.e. we are actually dealing with an "anti-bottleneck"—the reconnections transport an energy flux much larger than the one supplied from the larger scales. The anti-bottleneck is of course forbidden by the energy conservation, so we are forced to conclude that the transformation of the classical regime must happen already before the scale l_0 is reached, and the reconnections play a crucial role in this process.

Let us first analyze the tangle of vortex lines at $T = 0$ at the length scales much larger than the typical interline separation under the condition of a developed Kolmogorov cascade. Although understood intuitively, the ability of the system of quantized vortex lines to mimic the classical Kolmogorov cascade is not trivial. We start by a rigorous demonstration of this fact.

At $T = 0$, vortex lines are the only degrees of freedom and their dynamics are completely captured by the Biot-Savart equation (8). The latter can be rewritten in

classical terms of vorticity $\mathbf{w} = \operatorname{curl} \mathbf{v}$ in the momentum space, $\mathbf{w}_\mathbf{k} = \int \mathbf{w}(\mathbf{r}) \exp[-i\mathbf{k}\cdot \mathbf{r}]\, d^3r = \kappa \int \exp[-i\mathbf{k}\cdot\mathbf{s}]\, d\mathbf{s}$. The result is *identical* to the vorticity equation for a normal ideal incompressible fluid:

$$\frac{\partial \mathbf{w}_\mathbf{k}}{\partial t} = \mathbf{k} \times \int \frac{d^3q}{(2\pi)^3} q^{-2} \big[\mathbf{w}_{\mathbf{k}-\mathbf{q}} \times [\mathbf{w}_\mathbf{q} \times \mathbf{q}]\big]. \tag{70}$$

In view of (70) we can formulate the conditions, under which the vortex tangle must be automatically equivalent to classical ideal-incompressible-fluid turbulence: (i) the energy must be concentrated at a sufficiently small wavenumber scale $k_{\rm en} \ll l_0^{-1}$, and (ii) the decay scenario must be local in the momentum space, so that the quantized nature of vorticity is irrelevant for the long-wavelength behavior. These conditions are not restrictive: (i) is automatically satisfied if turbulence is generated by classical means due to the large compared to κ values of the velocity circulation, and (ii) is necessary for the existence of the Kolmogorov cascade in classical fluids as well.

Note that the circulation quantum κ completely drops out of the vorticity equation. This is a manifestation of the known fact that the superfluid hydrodynamics is completely described by the classical Euler equation with respect to which the quantization of circulation is nothing but an imposed initial condition enforced by quantum mechanics—due to the Kelvin theorem, once preformed the velocity circulation is a constant of motion. Since the dynamics of each individual vortex line are controlled by the circulation quantum κ, the independence of (70) on κ leads to an important conclusion that any large-scale (classical) motion necessarily implies strong coupling of the underlying vortex lines and that the crossover to the quantized regime is due to the self-induced motion of the vortex lines starting to dominate over the inter-line coupling. To obtain the corresponding crossover scale r_0, let us formally decompose the integral (4) into the self-induced part, $\mathbf{v}^{\rm SI}(\mathbf{s})$, for which the integration is restricted to the vortex line containing the element $\mathbf{s}$, and the remaining contribution induced by all the other lines $\mathbf{v}^{\rm I}(\mathbf{s})$,

$$\mathbf{v}(\mathbf{s}) = \mathbf{v}^{\rm SI}(\mathbf{s}) + \mathbf{v}^{\rm I}(\mathbf{s}). \tag{71}$$

By the definition of r_0, at length scales $r \gg r_0$ the turbulence mimics classical vorticity taking on the form of a dense coherently moving array of vortex lines bent at a curvature radius of order r. The velocity field of this configuration obeys the Kolmogorov law

$$v_r \sim (\varepsilon r)^{1/3}, \quad r \gg r_0, \tag{72}$$

where ε is the energy flux per unit mass of the fluid formed at the energy-containing eddies and transferred by the cascade. Here and below the subscript r means typical variation of a field over a distance $\sim r$. On the other hand, the value of v_r is fixed by the quantization of velocity circulation around a contour of radius r, namely $v_r r \sim \kappa n_r r^2$, where n_r is the areal density of vortex lines responsible for the vorticity at the scale r. Note that scale invariance requires that on top of vorticity at the scale r there be a fine structure of vortex bundles of smaller sizes, so that, mathematically, $n_r r^2$ is the difference between large numbers of vortex lines crossing the area of the contour

r in opposite directions. The quantity n_r is related to the flux by

$$n_r \sim \left[\frac{\varepsilon}{\kappa^3 r^2}\right]^{1/3}, \quad r \gg r_0. \tag{73}$$

The underlying dynamics of a single vortex line in the bundle is governed by v_r^{I} and v_r^{SI}. While by its definition $v_r^I \sim v_r$, which is given by (72), the self-induced part is determined by the curvature radius r of the vortex line according to the LIA, (11),

$$v_r^{\mathrm{SI}} \sim \Lambda_r \frac{\kappa}{r}, \tag{74}$$

where $\Lambda_r = \ln(r/a_*)$. Here and throughout this section, the logarithmic accuracy will be sufficient for the analysis, and, correspondingly, we replace Λ_r with $\Lambda = \ln(l_0/a_0)$. At length scales where $v_r^{\mathrm{I}} \gg v_r^{\mathrm{SI}}$, the vortex lines in the bundle move coherently with the same velocity $\sim v_r^{\mathrm{I}}$. However, at the scale $r_0 \sim (\Lambda^3\kappa^3/\varepsilon)^{1/4}$, the self-induced motion of the vortex line becomes comparable to the collective motion, $v_r^{\mathrm{SI}} \sim v_r^{\mathrm{I}}$. At this scale, individual vortex lines start to behave independently from each other and thus r_0 gives the lower cutoff of the inertial region of the Kolmogorov spectrum (72).

Since r_0 is the size of the smallest classical eddies, the areal density of the vortex lines at this scale is given by the typical interline separation, $n_{r_0} \sim 1/l_0^2$. In other words, vortex bundles at the scale r_0 consist of almost parallel vortex lines separated by the spacing l_0. With (73), we arrive at

$$r_0 \sim \Lambda^{1/2} l_0, \tag{75}$$

$$l_0 \sim (\Lambda\kappa^3/\varepsilon)^{1/4}. \tag{76}$$

The crossover can be also understood in slightly more visual terms. Let us introduce an effective number of vortex lines N_r in a bundle of size r. This number is obtained as an algebraic sum of the number of lines going through the bundle cross-section in opposite directions and is given by $N_r = n_r r^2 \sim \varepsilon^{1/3} r^{4/3}/\kappa$. In view of (72), (74), the number of lines in a bundle relative to Λ determines whether it behaves as a classical eddy or a set of independent vortex lines: $N_r \gg \Lambda$ means that the coupling between the vortex lines dominates resulting in the crossover when $N_{r_0} \sim \Lambda$. Thus, in the theoretical limit of $\Lambda \gg 1$ the bundles still contain a large number of vortex lines at the scale where the classical regime breaks down.

In the next subsection we shall introduce the cascade mechanism that supersedes the Kolmogorov cascade of eddies at the scales immediately adjacent to r_0.

5.2 Reconnections of Bundles

The analysis presented in this and the following section relies on the fact that the number of vortex lines in a bundle at the crossover scale is large, $N_{r_0} \gg 1$, which, in view of (75), is guaranteed in the limit of large Λ.

At the scale r_0, turbulence consists of randomly oriented vortex-line bundles of size r_0 formed by the classical regime. The length r_0 plays the role of a correlation radius in the sense that relative orientation of two vortex lines (with the short-wavelength structure smoothed out) becomes uncorrelated only if they are a distance

$\gtrsim r_0$ apart. On the other hand, the crossover to the quantized regime means that each line starts moving according to its geometric shape, as prescribed by (11). Therefore, reconnections, at least between separate bundles, are inevitable and, as we show below, capable of sustaining the flux ε.

The quantity that will play an important role in the analysis is the energy transferred to a lower scale after one reconnection of vortex lines at the scale k^{-1}, which, following Ref. [5], can be written as

$$\varepsilon_k \sim f(\gamma)\Lambda\rho\kappa^2 k^{-1}. \tag{77}$$

Here, $f(\gamma)$ is a dimensionless function of the angle γ at which the vortex lines cross ($\gamma = 0$ corresponds to parallel lines). Its asymptotic form is

$$f(\gamma) \sim \gamma^2, \quad \gamma \ll 1. \tag{78}$$

Although at the scale r_0 there is already no coupling between vortex lines to stabilize the bundles, they should still move coherently on the time scale of their turnover time since, by the definition of the bundle size r_0, geometry of neighboring lines at this scale is essentially the same over distances $\lesssim r_0$. On the other hand, during about one turnover the bundle must cross a neighboring bundle and reconnect providing a mechanism of energy transfer to the lower scales. It is possible, however, that vortex lines *within* the bundle reconnect. One can show that such processes can not lead to any significant redistribution of energy at the scale r_0 (but they will play an important role at smaller scales) and thus to a deformation of the bundle at this scale because they happen at small angles so that the energy (77) is too small. Indeed, the dimensional upper bound on the rate at which two lines at a distance $l \ll r_0$ can cross each other is, from (11), $\Lambda\kappa/r_0 l$, while the actual value should be much smaller due to the strong correlations between line geometries. Taking into account that the number of lines in the bundle is $(r_0/l_0)^2$ and that $\gamma \sim l/r_0$, the contribution to the energy flux from these processes is bounded by $(l/r_0)\varepsilon$. Only when $l \sim r_0$ the reconnections become important, which are the reconnections between the whole bundles of size r_0.

Crossing of the bundles results in reconnections between all their vortex lines and Kelvin waves with a smaller but adjacent wavelength λ are generated. This picture of bundle crossing was recently corroborated by direct numerical simulations [24]. The coherence of the initial bundles implies that the waves on different vortex lines of the same bundle must be generated coherently. Thus, at the scale $k^{-1} \lesssim r_0$, adjacent vortex lines should still be almost parallel with Kelvin waves on them of the wavenumber k and amplitudes b_k—vortex lines at the scale k^{-1} also form bundles. Similarly, these bundles can reconnect transporting the energy to a lower scale, where similar bundle reconnections happen, and so on down the scales until the bundle size is comparable to the interline distance and the self-similar regime is cut off.

An important ingredient of this scenario characterizing the bundles at a scale k^{-1} is the correlation radius $r_k^{(c)}$ of the vortex-line geometry (with the short-wavelength structure smoothed out up to k^{-1}) in the transverse to the bundle direction. The value of $r_k^{(c)}$ determines the distance over which neighboring vortex lines can be considered as parallel, i.e. it gives the transverse size of the bundle. This size is due to a finite

time required for the Kelvin-wave amplitude at the scale k_2^{-1} to build up (after a reconnection at a larger scale $k_1^{-1} > k_2^{-1}$), which is of order of the wave turnover time, $\tau_{k_2} \sim 1/\kappa\Lambda k_2^2$. The Kelvin waves that were generated within the time $\sim\tau_{k_2}$ are coherent. In other words, as a reconnection of two lines happens at time $t = \tau_{k_2}$ at the scale $k_1^{-1} > k_2^{-1}$, the lines that reconnected in the same bundle at $t = 0$ have already-developed waves, which can not be coherent with the waves about to be generated at $t \gtrsim \tau_{k_2}$. Thus, the distance traveled by the bundle at the scale k_1^{-1} over the time $\sim\tau_{k_2}$ determines the orientational correlation radius at the scale k_2, $r_{k_2}^{(c)} = r_{k_2}^{(c)}(k_1) = b_{k_1}k_1^2/k_2^2$. Since the scales k_1 and k_2 are actually adjacent (i.e. different only by a factor of order unity), we finally get $r_k^{(c)} \sim b_k$.

The spectrum of Kelvin waves b_k in this regime can be obtained from the condition $\tilde{\varepsilon}_k \equiv \varepsilon$, where $\tilde{\varepsilon}_k$ is the energy flux per unit mass transported by the reconnections at the scale k^{-1},

$$\tilde{\varepsilon}_k \sim \left(k/\rho[r_k^{(c)}]^2\right) N_k \varepsilon_k \tau_k^{-1}. \tag{79}$$

Here, we take into account that the correlation volume of the reconnection is $[r_k^{(c)}]^2/k$, $N_k \sim (b_k/l_0)^2$ is the number of vortex lines participating in the reconnection, and $\tau_k^{-1} \sim \kappa\Lambda k^2$ is the rate at which the bundles cross. Physically, b_k determines the typical crossing angle, $\gamma \sim b_k k$, thereby controlling the energy lost in one reconnection. From (79), the spectrum of Kelvin waves in the bundle-crossing regime has the form

$$b_k \sim r_0^{-1}k^{-2}. \tag{80}$$

At the wavelength $\sim\lambda_\mathrm{b} = \Lambda^{1/4}l_0$, the amplitudes become of order of the interline separation $b_k \sim l_0$ and the notion of bundles looses meaning—the cascade of bundles is cut off. The scenario at the scales $\lambda \lesssim \lambda_\mathrm{b}$ is rather peculiar and the next subsection is devoted to its description.

5.3 Reconnections of Adjacent Lines

In the regime of bundle crossings, in view of (80), the Kelvin-wave amplitudes are steeply decreasing with the wavenumber, so that at the wavelength $\lambda_\mathrm{b} = \Lambda^{1/4}l_0$, where the amplitudes become of order of the interline spacing l_0, the vortex lines are only slightly bent, $b_k k \ll 1$. This poses an interesting question of what is driving the cascade at the wavelengths below λ_b. Since the amplitude spectrum can not change discontinuously, at the scales adjacent to λ_b we must still have $b_k k \ll 1$, so that the mechanism of self-reconnections is strongly suppressed. On the other hand, the kinetic times of the purely non-linear regime are still too long to carry the flux ε [13]. We thus conclude that in some range of length scales $\lambda_\mathrm{c} \lesssim \lambda \lesssim \lambda_\mathrm{b}$ there should take place a build up of the relative Kelvin-wave amplitude supported by the energy flux from the scale λ_b until $b_k k \sim 1$ and the self-reconnections can take over the cascade, the amplitudes b_k being defined by the condition of constant energy flux per unit length and the crossover scale λ_c being associated with the condition $b_{k\sim 1/\lambda_\mathrm{c}} \sim \lambda_\mathrm{c}$. The observation crucial for understanding the particular mechanism of this regime and thus finding b_k is that each nearest-neighbor reconnection (happening at the rate

$\propto \Lambda/\lambda_b^2$ per each line element of the length $\sim\lambda_b$) performs a sort of *parallel processing* of the energy distribution for *each* of the wavelength scales in the range $[\lambda_c, \lambda_b]$. For the given wavelength scale $\lambda \sim k^{-1}$, the energy transferred by a single collision is $\propto \Lambda(b_k k)^2\lambda$, and with the above estimate of the collision rate per the length λ_b, this readily yields the spectrum

$$b_k \sim l_0(\lambda_b k)^{-1/2}, \tag{81}$$

and, correspondingly, $\lambda_c \sim l_0/\Lambda^{1/4}$. Note that the rise of the relative amplitude $b_k k \propto k^{1/2}$ implied by (81) describes the process of fractalization of the vortex lines with its culmination around the scale λ_c. Thus, in this regime, the energy is actually contained at the low-end of the inertial range. We refer to this circumstance as a *deposition* of energy and discuss the relevance of this term in Sect. 7. Although the deposition of energy makes this regime formally different from a standard cascade setup, its presence has no effect on the rest of the inertial range and thus on the overall cascade efficiency.

5.4 To the Kelvin-Wave Cascade

The stages of vortex-bundle reconnections and the reconnections between adjacent vortex lines essentially complete the transformation of the quasi-classical tangle that is necessary to connect the classical regime to the Kelvin-wave cascades on individual vortex lines. At the wavelengths $\sim\lambda_c$ the self-reconnections on the vortex lines take over the cascade and the picture at the shorter scales is qualitatively not different from that of the non-structured tangles. The self-reconnection regime continues in the range $\lambda_* \ll \lambda \ll \lambda_c$ with the spectrum $b_k \sim k^{-1}$. At a sufficiently small wavelength λ_*, the strongly turbulent cascade of Kelvin waves is replaced by the purely non-linear cascade. The spectrum of Kelvin-wave amplitudes in the non-linear cascade is given by (53). The value of λ_* can be determined by matching the energy flux ε with $\Theta/\rho l_0^2$, where $b_{k\sim 1/\lambda_*} \sim k^{-1} \sim \lambda_*$. With (76), we then obtain

$$\lambda_* = l_0/\Lambda^{1/2}. \tag{82}$$

At $T = 0$ Kelvin waves decay emitting phonons. This dissipation mechanism is negligibly weak all the way down to wavelengths of order $\lambda_{\mathbf{ph}}$, where the rate of energy radiation by the vortex lines becomes comparable to ε. As we show in Sect. 6 this condition with the estimate for the power of sound radiation by kelvons yields

$$\lambda_{\mathrm{ph}} \sim \Lambda^{27/31}\left[\kappa/cl_0\right]^{25/31} l_0. \tag{83}$$

The scale $\lambda_{\mathbf{ph}} \lll \lambda_*$ gives the lower dissipative cutoff of the Kelvin-wave cascade.

The overall decay scenario is summarized in Fig. 3, where we plot the resulting Kelvin-wave spectrum in the whole quantized regime.

5.5 Scanning by Finite Temperature

In this subsection, on the basis of the presented decay scenario at $T = 0$, we describe a theory of the low-temperature dissipative cutoff of the cascade [15]. We shall

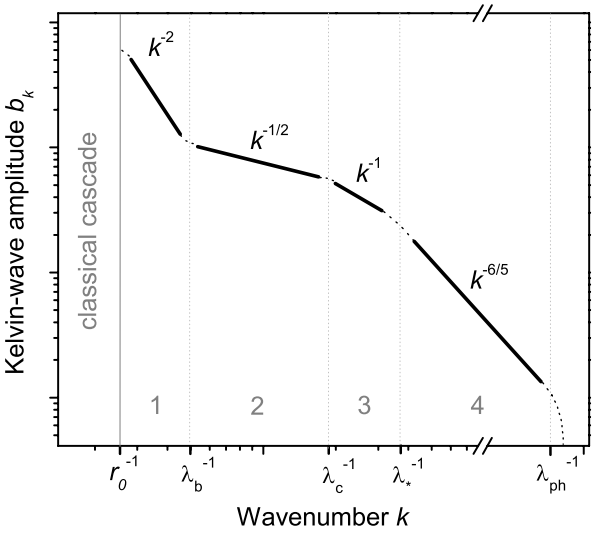

Fig. 3 Spectrum of Kelvin waves in the quantized regime of quasi-classical tangles. The inertial range consists of a chain of cascades driven by different mechanisms: (*1*) reconnections of vortex-line bundles, (*2*) reconnections between nearest-neighbor vortex lines in a bundle, (*3*) self-reconnections on single vortex lines, (*4*) non-linear dynamics of single vortex lines without reconnections

demonstrate that the temperature dependence of the total vortex-line length density L comes from the dependence of the wavelength scale λ_{cuttoff}, at which the cascade ceases due to the mutual friction of vortex lines with the normal component, on the dimensionless friction coefficient $\alpha \propto T^5 \ \ (T \to 0)$. The main result of the theory is the prediction for the function $\ln L(\ln \alpha)$, which turns out to have a very characteristic form reflecting the four qualitatively distinct wavenumber regions of the cascade in the quantized regime. The results of the theory are in an excellent agreement with the recent experiments by Walmsley et al. [18, 23] giving a strong evidence for the highly nontrivial scenario of low-temperature turbulence decay.

If the vortex lines were smooth, the vortex-line density L would be simply related to the interline separation as $L = l_0^{-2}$. However, the presence of a fine wave structure on the lines can make the total length many times as large as l_0^{-2} (or even infinite in the limit of fractal lines). The increase of L due to the presence of KWs is related to their spectrum by [5] (cf. (59))

$$\ln\bigl[L(\alpha)/L_0\bigr] = \int_{\tilde{k}}^{k_{\text{cutoff}}(\alpha)} (b_k k)^2 dk/k. \tag{84}$$

Here $k_{\text{cutoff}} \sim 1/\lambda_{\text{cutoff}}$, $\tilde{k}$ is the smallest wavenumber of the KW cascade (not to be confused with the smallest wavenumber of the Kolmogorov cascade) at which the concept of a definite cutoff scale is meaningful, and L_0 is the "background" line density corresponding to $k_{\text{cutoff}} \sim \tilde{k}$. There is an ambiguity in the definition of b_k associated with the choice of the spectral width of the scale k, which is fixed in (84) by setting the proportionality constant on each side to unity.

At $T = 0$, the cascade is cut off by the radiation of sound (at least in ^{4}He) at the length scale $\lambda_{\text{cutoff}} = \lambda_{\text{ph}}$ given by (83). Changing the temperature one controls $\lambda_{\text{cutoff}}(T) > \lambda_{\text{ph}}$ in (84), which allows one to *scan* the KW cascade observing qualitative changes in $L(T)$ as λ_{cutoff} traverses different cascade regimes. The existence

of a well-defined cutoff is due to the fact that the cascade is supported by rare kinetic events in the sense that the collision time $\tau_{\rm coll} \equiv \tau_{\rm coll}(\varepsilon, k)$ is much larger than the KW oscillation period, $\tau_{\rm per} \equiv \tau_{\rm per}(k)$. The dissipative time $\tau_{\rm dis} \equiv \tau_{\rm dis}(\alpha, k) \sim \tau_{\rm per}/\alpha$, as we show below, is the typical time of the frictional decay of a KW at the scale k. Thus, the cutoff condition is $\tau_{\rm dis}(\alpha, k) \sim \tau_{\rm coll}(\varepsilon, k)$, which implies that the energy dissipation rate at a given wavenumber scale becomes comparable to the energy being transferred to higher wavenumber scales per unit time by the cascade. It is this condition that defines the cutoff wavenumber $k_{\rm cutoff} \equiv k_{\rm cutoff}(\varepsilon, \alpha)$. Decreasing T and thus $\alpha(T)$, one gradually increases $k_{\rm cutoff}$, thereby scanning the cascade. In view of (84), this in principle allows one to extract the KW spectrum.

At finite T, dissipative dynamics of a vortex line element are described by the equation (omitting the third term in the r.h.s., which is irrelevant for dissipation) [1, 2]

$$\dot{\mathbf{s}} = \mathbf{v}(\mathbf{s}) + \alpha \mathbf{s}' \times \big[\mathbf{v}_{\rm n}(\mathbf{s}) - \mathbf{v}(\mathbf{s})\big]. \tag{85}$$

Here $\mathbf{v}(\mathbf{r})$ is the superfluid velocity field, $\mathbf{v}_{\rm n}(\mathbf{r})$ is the normal velocity field, $\mathbf{s} = \mathbf{s}(\xi, t)$ is the time-evolving radius-vector of the vortex line element parameterized by the arc length, the dot and the prime denote differentiation with respect to time and the arc length, respectively.

At $\alpha \sim 1$ the superfluid and normal components are strongly coupled and the KWs are suppressed. In this case, the cascade must cease before it enters the quantized regime, i.e. $\lambda_{\rm cuttoff} \gtrsim r_0$. If, however, the mutual friction is small, then $\alpha^{-1} \gg 1$ gives the characteristic number of KW oscillations required for the wave to decay. Indeed, to the first approximation in $1/\Lambda$, $\mathbf{v}(\mathbf{s})$ in (85) is given by the local induction approximation (11). In the range $\lambda \ll r_0$, which we will be interested in, the normal component is already laminar and thus the field $\mathbf{v}_{\rm n}$ has no structure at these small scales. In addition, as long as $\alpha \ll 1$, the disturbance of the normal component caused by vortex line motion as these scales can be neglected. Therefore, $\mathbf{v}_{\rm n}(\mathbf{s})$ can be treated as a constant in (85), which makes it irrelevant for KW dissipation. In this case, (85), (11) give the rate at which the amplitude b_k of a KW with the wavenumber k decays due to the mutual friction,

$$\dot{b}_k \sim -\alpha \omega_k b_k, \tag{86}$$

while the KW dispersion is $\omega_k = (\kappa/4\pi)\Lambda k^2$. Here and below we omit factors of order unity, which are subject to the definition of the spectral width of the wave. These factors can not be found within our theory, but can be extracted from experimental data (as we do it below) and from numerical simulations. Since the energy per unit line length associated with the wave is $E_k \sim \kappa \rho \omega_k b_k^2$, the power dissipated (per unit line length) at the scale $\sim k^{-1}$ is given by

$$\Pi(k) \sim \alpha \kappa \rho \omega_k^2 b_k^2, \tag{87}$$

where ρ is the fluid density. In the following, we analyze ST as $\alpha(T)$ scans through the regimes summarized in Fig. 3.

Regime (1) At this stage the vortex lines are organized in bundles; the amplitudes of waves on these lines are given by (80). One can estimate the total power lost due to the friction of these bundles at the wavenumber scale $r_0^{-1} \ll k \ll k_\mathrm{b} \sim \lambda_\mathrm{b}^{-1}$ per unit mass of the fluid as

$$\varepsilon_\mathrm{dis}(k) = \frac{1}{\rho b_k^2} \frac{b_k^2}{l_0^2} \Pi(k) \sim \alpha \kappa^3 \Lambda / l_0^4. \tag{88}$$

Here, the first factor in the r.h.s. is associated with the correlation volume at this scale $\sim b_k^2 k^{-1}$ and the second one stands for the number of vortex lines in the volume. Note that the dissipated power is constant at all the length scales within this regime and, since the interline separation is related to the Kolmogorov flux by (76), it is simply given by $\alpha\varepsilon$. Thus, when $\alpha \ll 1$ the kinetic channel in the whole regime (1) becomes efficient and the cascade reaches the scale λ_b, where the notion of bundles becomes meaningless. That is, the regime (1), as opposed to the regimes (2)–(4), is *not* actually scanned by α—its inertial range develops as a whole while α evolves from $\alpha \sim 1$ to $\alpha \ll 1$. [In the purely theoretical limit of exponentially large Λ, when the inertial range of the regime (1) occupies many decades, a (loose) dissipative cutoff appears in the regime (1) as well; the cutoff wavelength in this case can be roughly estimated as $\ln(r_0/\lambda_\mathrm{cutoff}) \sim 1/\alpha$.]

Regime (2) In the range $k_\mathrm{b} \ll k \ll k_\mathrm{c} \sim \lambda_\mathrm{b}^{-1}$, the spectrum of KWs is given by $b_k \sim l_0 (k_\mathrm{b}/k)^{1/2}$ ((80)) which for the dissipated power yields

$$\varepsilon_\mathrm{dis}(k) \sim \frac{1}{\rho l_0^2} \Pi(k) \sim \alpha \kappa^3 \Lambda^{7/4} k^3 / l_0. \tag{89}$$

The condition $\varepsilon_\mathrm{dis}(k) \sim \varepsilon$ gives the cutoff wavenumber

$$k_\mathrm{cutoff} = \xi_2 \Lambda^{-1/4} \alpha^{-1/3} (2\pi / l_0), \quad k_\mathrm{b} \ll k_\mathrm{cutoff} \ll k_\mathrm{c}, \tag{90}$$

where ξ_2 is some constant of order unity. Then, from (84) we obtain

$$\ln \frac{L(k_\mathrm{cutoff})}{L_0} = C^2 (k_\mathrm{b} l_0)^2 [k_\mathrm{cutoff}/k_\mathrm{b} - 1]. \tag{91}$$

Here, we set $b_k = C l_0 (k_\mathrm{b}/k)^{1/2}$, where C is a constant of order unity. The overall magnitude of b_k in the other regimes follows then from the continuity.

Regime (3) In this regime, supported by self-reconnections, the spectrum is given by $b_k \sim k^{-1}$ (up to a logarithmic prefactor). The corresponding energy balance condition yields the cutoff scale:

$$k_\mathrm{cutoff} = \xi_3 (\Lambda\alpha)^{-1/2} (2\pi / l_0), \quad k_\mathrm{c} \ll k_\mathrm{cutoff} \ll k_*. \tag{92}$$

With the logarithmic prefactor taken into account, (66), the spectrum in this regime reads $b_k = C[1 + c_3^2 \ln(k/k_\mathrm{c})]^{-1/2} (\sqrt{k_\mathrm{c} k_\mathrm{b}}/k) l_0$, where c_3 is a constant of order unity. Then the relative increase of vortex line density through this regime is given by

$$\frac{L(k_\mathrm{cutoff})}{L(k_\mathrm{c})} = \left[1 + c_3^2 \ln \frac{k_\mathrm{cutoff}}{k_\mathrm{c}} \right]^\nu, \tag{93}$$

where $\nu = C^2 k_c k_b l_0^2 / c_3^2$.

Regime (4) Since the spectrum of the purely nonlinear regime, $b_k \sim k^{-6/5}$, (53) is steeper than the marginal $b_k \sim k^{-1}$ meaning that the integral in (84) builds up at the lower limit, as soon as $k_{\mathrm{cutoff}} \gtrsim k_*$ the line density $L(k_{\mathrm{cutoff}})$ starts to saturate and becomes independent of k_{cutoff} at $k_{\mathrm{cutoff}} \gg k_*$. The energy balance gives the dependence $k_{\mathrm{cutoff}}(\alpha)$,

$$k_{\mathrm{cutoff}} = \xi_4 \Lambda^{-3/4} \alpha^{-5/8} (2\pi / l_0), \quad k_{\mathrm{cutoff}} \gg k_*, \tag{94}$$

where ξ_4 is an unknown constant. The coefficient in the KW spectrum is fixed by continuity with the previous regime, yielding $b_k = C[1 + c_3^2 \ln(k_*/k_c)]^{-1/2} \sqrt{k_c k_b} k_*^{1/5} \cdot k^{-6/5} l_0$. Equation (84) thus yields

$$\frac{L(k_{\mathrm{cutoff}})}{L(k_*)} \approx 1 + \frac{(5C^2/2) k_c k_b l_0^2}{1 + c_3^2 \ln(k_*/k_c)} \left[1 - \left(\frac{k_*}{k_{\mathrm{cutoff}}} \right)^{2/5} \right]. \tag{95}$$

The continuity of k_{cutoff} leads to the following constraints on the free coefficients in (90), (92), and (94), $\xi_3 = \xi_2 \Lambda^{1/4} \alpha_c^{1/6}$, $\xi_4 = \xi_2 \Lambda^{1/2} \alpha_c^{1/6} \alpha_*^{1/8}$, where $\alpha_c \sim \Lambda^{-3/2}$ is the value of the friction coefficient at which the cascade is cut off at the crossover between the regimes (2) and (3) and $\alpha_* \sim 1/\Lambda^2$ corresponds to the one between (3) and (4). Introducing $\alpha_b \lesssim 1$, corresponding to the crossover from the regime (1) to (2), we rewrite (91), (93), and (95) in terms of α:

$$\begin{aligned}
&\ln \frac{L(\alpha)}{L_0} = A_2 \left[(\alpha_b/\alpha)^{1/3} - 1 \right], \quad \alpha_c \ll \alpha \ll \alpha_b, \\
&\frac{L(\alpha)}{L(\alpha_c)} = \left[1 + (c_3^2/2) \ln \frac{\alpha_c}{\alpha} \right]^{\nu}, \quad \alpha_* \ll \alpha \ll \alpha_c, \\
&\frac{L(\alpha)}{L(\alpha_*)} \approx 1 + A_4 \left[1 - \left(\frac{\alpha}{\alpha_*} \right)^{1/4} \right], \quad \alpha \ll \alpha_*,
\end{aligned} \tag{96}$$

where

$$\begin{aligned}
&A_2 = (2\pi)^2 \xi_2^2 C^2 / \Lambda^{1/2} \alpha_b^{2/3}, \\
&\nu = (2\pi)^2 \xi_2^2 C^2 / \Lambda^{1/2} (\alpha_c \alpha_b)^{1/3} c_3^2, \\
&A_4 = 5(2\pi)^2 \xi_2^2 C^2 / 2\Lambda^{1/2} [1 + (c_3^2/2) \ln(\alpha_c/\alpha_*)] (\alpha_c \alpha_b)^{1/3}.
\end{aligned} \tag{97}$$

Although the excellent quantitative agreement with the experiments can be sceptically attributed to the large number of fitting parameters, it is remarkable that the nontrivial qualitative behavior of $L(\alpha)$ exhibits the form peculiar to our decay scenario (see Fig. 4). As α decreases from $\alpha \sim 1$ to the values significantly smaller than unity, the line density L increases only by some factor close to unity ($\sim$1.5 in the experiment), which reflects the formation of the regime (1) driven by the reconnections of vortex bundles. During the crossover from the region (1) to (2), the increase of L is minimal—a *shoulder* in the curve $L(\alpha)$ arises. It is only well inside the region

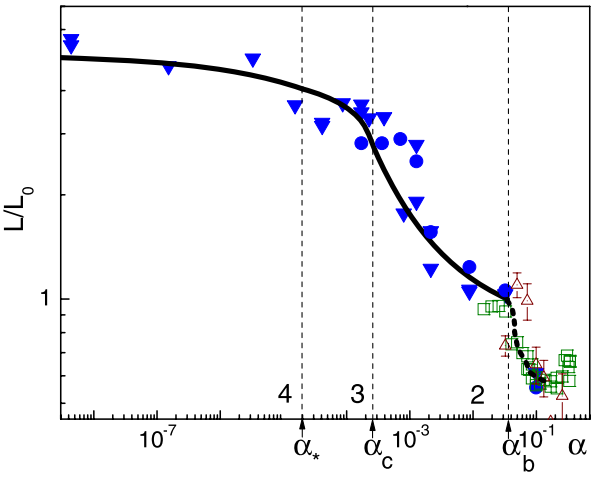

Fig. 4 (Color online) Fit of the experimental data (*closed circles* and *triangles*) adapted from Ref. [23] ($l_0 \approx 5 \times 10^{-3}$ cm giving $\Lambda \approx 13$). The high temperature measurements of Refs. [39, 40] are represented by *open squares* and *open triangles* respectively. The form of $\alpha(T)$ is taken according to Ref. [53] at $T \gtrsim 0.5$ K (roton scattering) and according to Ref. [45] at $T \lesssim 0.5$ K (phonon scattering). The fitting parameters are $A_2 \approx 0.25$, $A_4 \approx 0.26$, $c_3 \approx 3.0$, $\nu \approx 0.14$ with $\alpha_b \approx 3.5 \times 10^{-2}$, $\alpha_c \approx 2.5 \times 10^{-4}$, $\alpha_* \sim 2.0 \times 10^{-5}$

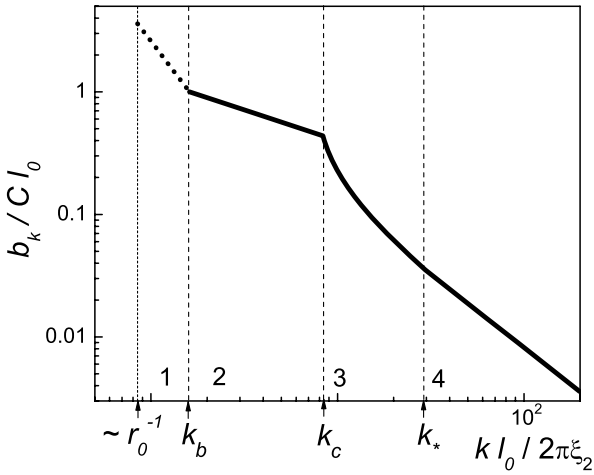

Fig. 5 Spectrum of Kelvin waves in the quantized regime quantified, apart from the regime (1), by the fit to experimental data, Fig. 4. In view of (84), the constants C and ξ_2 can be found only in the combination $\xi_2 C \approx 0.049$. The regimes (1)–(4) correspond to those in Fig. 3

(2) that the increase of L becomes progressively pronounced, and, at the crossover to the region (3), the function $L(\alpha)$ achieves its maximal slope, determined by the developed fractalization of the vortex lines necessary to support the cascade within the interval (3). As the cutoff moves along the interval (3) towards higher wavenumbers, the slope of $L(\alpha)$ becomes less steep due to the logarithmic decrease of the characteristic amplitude of KW turbulence. When the cutoff passes the crossover to the regime (4), the curve $L(\alpha)$ gradually levels. (Note that because of the closeness of the KW spectra in the regimes (3) and (4) the crossover between them, as expected, is not distinct, which results in a significant uncertainty in the choice of α_*.) Fitting the experimental data fixes the values of the dimensionless parameters, thus revealing the *quantitative* form of the KW spectrum shown in Fig. 5. Note, however, that in view of the fact that the experimental $\Lambda \sim 10$ is not so large we would expect certain systematic deviations, but a significant scatter of the experimental data does not allow us to assess them.

6 Kelvon-Phonon Interaction

6.1 Hydrodynamic Action. Hamiltonian of Kelvon-Phonon Interaction

The general problem of kelvon interaction with other modes is relevant far beyond the scope of superfluid turbulence. Since the early study of phonon scattering by vortex lines [54], much interest has been attracted by the problems of the interaction of Kelvin waves with density-distortion modes [8, 10, 50, 55–57]. In neutron stars, the excitation of Kelvin waves due to the interaction with the nuclei in the solid crust is suggested to be the main mechanism of pulsar glitches [50]. Nonlinear kelvon dynamics is also becoming an attractive topic in the field of ultra-cold gases, where one can study kelvon coupling to the modes of the Bose-Einstein condensate *in situ*, as, e.g., in the problem of kelvon excitation by the quadrupole mode [55–57].

In this section we describe a systematic approach (developed by the authors in Ref. [15]) to the problem of interaction of phonons with vortices in the hydrodynamic regime, i.e. when any physical length scale is much larger than the vortex core size a_0, which allows one to describe vortices as geometrical lines [1]. We derive the interaction Hamiltonian basing the analysis on the small parameter

$$\beta = a_0 \tilde{k} \ll 1, \tag{98}$$

where $\tilde{k}$ is the largest wave number among kelvons and phonons. To employ the transparent description in terms of the normal modes, we confine ourselves to the case of weak nonlinearity, which for kelvons implies the small parameter α, (30), meaning that the amplitudes b_k of the Kelvin waves of the typical wavelength $\lambda \sim k^{-1}$ are much smaller than λ, $\alpha_k = b_k k \ll 1$. For phonons this requires that $\eta \ll n$, where η is the number density fluctuation in a sound wave and n is the average number density. The obtained result allows us to rigorously describe the radiation of sound by kelvons, which we apply to the problem of superfluid turbulence decay at zero temperature in the next subsection.

Let us first describe the qualitative ideas behind the derivation. The condition (98) implies that the typical vortex-line velocities are much smaller than the speed of sound. Along with $\eta \ll n$ it leads to the fact that the vortex-phonon coupling contributes only small corrections to the dynamics of the non-interacting vortex and phonon subsystems. Therefore, a perturbative approach is applicable, provided the interaction energy is written in terms of the canonical variables. Normally, the form of the canonical variables comes from the solution of the interaction-free dynamics. However, when studying vortices separate from phonons, one naturally neglects the compressibility of the fluid, which we did in Sect. 2, since finite compressibility leads only to higher-order "relativistic" corrections to vortex dynamics. As a result, the dynamics of vortices are described by the Hamiltonian (29), written in terms of the geometrical configuration of the vortex lines. When the vortices are absent, the phonon modes come from the bilinear Hamiltonian for the density fluctuation $\eta(\mathbf{r}, t)$ and the phase field $\varphi(\mathbf{r}, t)$, which determines the velocity in the density wave (see, e.g., [58]). If finite compressibility of a superfluid is taken into account in order to join the subsystems, the positions of vortices and the fields $\eta(\mathbf{r}, t), \varphi(\mathbf{r}, t)$ are no longer the sets of canonical variables because of the variable-mixing term in the Lagrangian.

This makes this perturbative problem quite peculiar since introducing the interaction, one has to simultaneously reconsider the canonical variables.

One can easily see that the standard vortex parametrization used in Sect. 2 fails to capture the physics of vortices when phonons are present. In (4), the geometrical position of the vortex lines unambiguously determines the instantaneous velocity field configuration at arbitrary distances, which is inconsistent with the finite velocity of propagation of excitations in a compressible medium. From this simple physical argument, we can already guess the form of the canonical variables: the long-distance part of the velocity field produced by vortices in (4) should actually belong to phonons.

The small parameters allow us to obtain an asymptotic expansion of the canonical variables by means of a systematic iterative procedure. Physically, the procedure restores the retardation in the adjustment of the superfluid velocity field to the evolving vortex configuration. It qualitatively changes the structure of the Hamiltonian with respect to the terms responsible for the radiation of sound and the relativistic corrections to the vortex dynamics.

Hydrodynamic Lagrangian: standard parametrization. Long-wave superfluid dynamics at zero temperature are described by the Popov's hydrodynamic action [59]:

$$S = \int dt\, d^3r \left[-(n+\eta)\dot{\Phi} - \frac{(n+\eta)}{2m_0}|\nabla\Phi|^2 - \frac{1}{2\varkappa}\eta^2 \right]. \tag{99}$$

Here the spatial integral is taken over the macroscopic fluid volume, $\Phi(\mathbf{r},t)$ is the phase field, which determines the velocity according to $\mathbf{v} = (1/m_0)\nabla\Phi$ ($\hbar = 1$), m_0 is the mass of a particle, $\varkappa$ is the compressibility, the dot denotes the derivative with respect to time, and the microscopic length scale is defined by $a_0 = \sqrt{\varkappa/nm_0}$. The vortex core radius is of order a_0.

The phase Φ is non-single-valued and contains topological defects, the vortex lines. The velocity circulation around each vortex line is quantized:

$$\oint \nabla\Phi(\mathbf{r}) \cdot d\mathbf{r} = 2\pi. \tag{100}$$

The defects can be separated from the regular contribution:

$$\Phi = \Phi_0 + \varphi, \tag{101}$$

where Φ_0 is non-single-valued and satisfies (100), while φ is regular and $\nabla\varphi$ is circulation-free. The standard decomposition into vortices and phonons is done by introducing an additional constraint that to the zeroth approximation eliminates the coupling between Φ_0 and φ in the Hamiltonian, namely

$$\Delta\Phi_0(\mathbf{r}) = 0. \tag{102}$$

(Physically, this parametrization is suggested by the velocity potential of an incompressible fluid.) With (101), (102) the Lagrangian becomes

$$L = \int d^3r \left[-n\dot{\Phi}_0 - \eta\dot{\varphi} - \eta\dot{\Phi}_0 \right] - H, \tag{103}$$

where $H = H_{\rm vor} + H_{\rm ph} + H'_{\rm int}$,

$$H_{\rm vor} = \frac{n}{2m_0}\int d^3r\big|\nabla\Phi_0\big|^2, \tag{104}$$

$$H_{\rm ph} = \int d^3r\bigg[\frac{n}{2m_0}\big|\nabla\varphi\big|^2 + \frac{1}{2\varkappa}\eta^2\bigg], \tag{105}$$

$$H'_{\rm int} = \frac{1}{2m_0}\int d^3r\Big[\eta\big|\nabla\Phi_0\big|^2 + 2\eta\nabla\varphi\cdot\nabla\Phi_0\Big]. \tag{106}$$

The coupling between the vortex variable, Φ_0, and the density waves, $\{\eta,\varphi\}$, is determined by $H'_{\rm int}$ and the time derivative term $\int d^3r\eta\dot\Phi_0$, both being first-order corrections to the non-interacting parts.

Noninteracting case. Following standard perturbative procedure, we first neglect the coupling between the vortex and phonons to find the non-interacting normal modes. The vortex part of the Lagrangian is then given by $L_{\rm vor} = -n\int d^3r\dot\Phi_0 - H_{\rm vor}$. For the sake of simplicity, from now on we consider a solitary vortex line; the generalization is straightforward. Let the two-dimensional vector $\boldsymbol{\rho}_0(z_0) = (x_0(z_0), y_0(z_0), 0)$ describe the position of the vortex line in the plane $z = z_0$ of a Cartesian coordinate system, where the z-direction is chosen along the vortex line. The field Φ_0 is a functional of $\boldsymbol{\rho}_0(z)$, hence

$$\int d^3r\dot\Phi_0 = \int dz\dot{\boldsymbol{\rho}}_0\cdot\frac{\delta}{\delta\boldsymbol{\rho}_0}\int d^3r\Phi_0. \tag{107}$$

To obtain $\int d^3r\dot\Phi_0$, it is sufficient to calculate the integral $\int d^3r\delta\Phi_0$, where $\delta\Phi_0$ is the variation of the phase field due to the distortion of the vortex line by $\delta\boldsymbol{\rho}_0(z)$. Using the identity $\Delta(\boldsymbol{\rho}^2) = 4$, with $\boldsymbol{\rho} = (x, y, 0)$, and (102), obtain

$$\int d^3r\delta\Phi_0 = \frac{1}{4}\int d^3r\nabla\cdot\big[\delta\Phi_0\nabla(\boldsymbol{\rho}^2)\big]. \tag{108}$$

The variation $\delta\Phi_0(\mathbf{r})$ can be viewed as being produced by two vortex lines with opposite circulation quanta and separated by $\delta\boldsymbol{\rho}_0(z)$. In view of (100) the field $\delta\Phi_0(\mathbf{r})$ experiences a jump of 2π across the surface $\mathcal{S}$ that extends between these vortex lines along the vector field $\delta\boldsymbol{\rho}_0(z)$, therefore the integration volume must have a cut along $\mathcal{S}$. Applying the Gauss theorem, we rewrite (108) as the surface integral $(1/2)\oint_{\mathcal{S}}\delta\Phi_0(\boldsymbol{\rho}\cdot d\mathbf{S})$ yielding

$$\int d^3r\dot\Phi_0 = \pi\int dz[\hat{\mathbf{z}}\times\boldsymbol{\rho}_0(z)]\cdot\dot{\boldsymbol{\rho}}_0(z). \tag{109}$$

Introducing the complex variable $w(z) = \sqrt{nm_0\kappa/2}[x(z)+iy(z)]$, where $\kappa = 2\pi/m_0$ is the velocity circulation quantum, obtain

$$L_{\rm vor} = \frac{1}{2}\int dz\big[iw^*\dot w - i\dot w^* w\big] - H_{\rm vor}[w, w^*], \tag{110}$$

which implies that $w(z)$ and $w^*(z)$ are the canonical variables with respect to $L_{\rm vor}$. The energy (104), rewritten in terms of $w(z)$ and $w^*(z)$ gives the vortex Hamiltonian (20), or the pseudo-Hamiltonian (29) with an appropriate regularization. We need only the bilinear term of the expanded with respect to $\alpha_k \ll 1$ Hamiltonian since the kelvon interactions are irrelevant for our problem. We change the notation for the kelvon spectrum reserving ω_q for phonons:

$$H_{\rm vor} \approx \sum_k \varepsilon_k a_k^\dagger a_k, \quad \varepsilon_k = \frac{\kappa}{4\pi}\big[\ln(1/ka_0) + C_0\big]k^2, \tag{111}$$

with a_k and $a_k^\dagger$ defined in Sect. 2. The sound waves are described by the Lagrangian $L_{\rm ph} = \int d^3r(-\eta\dot\varphi) - H_{\rm ph}[\eta,\varphi]$, with $H_{\rm ph}$ given by (105). We assume that the system is contained in a cylinder of radius R with the symmetry axis along the z-direction and that the system is periodic along z with the period L. In the cylindrical geometry, the phonon fields $\eta(r,\theta,z)$, $\varphi(r,\theta,z)$ are parametrized by phonon creation and annihilation operators c_s, $c_s^\dagger$ as

$$\begin{aligned}
\eta &= \sum_s \sqrt{\omega_s \varkappa/2}\big[\chi_s c_s + \chi_s^* c_s^\dagger\big],\\
\varphi &= -i\sum_s \sqrt{1/2\omega_s\varkappa}\big[\chi_s c_s - \chi_s^* c_s^\dagger\big],\\
\chi_s &= \chi_s(r,\theta,z) = \mathcal{R}_{mq_r}(r)Y_m(\theta)\mathcal{Z}_{q_z}(z),
\end{aligned} \tag{112}$$

where $\mathcal{R}_{mq_r}(r) = (\pi q_r/R)^{1/2}J_m(q_r r)$, $Y_m(\theta) = (2\pi)^{-1/2}\exp(im\theta)$, $\mathcal{Z}_{q_z}(z) = L^{-1/2}\exp(iq_z z)$, s stands for $\{q_r, m, q_z\}$, and $J_m(x)$ are the Bessel functions of the first kind. The phonon Hamiltonian then reads

$$H_{\rm ph} = \sum_s \omega_s c_s^\dagger c_s, \quad \omega_s = cq, \tag{113}$$

with $q = \sqrt{q_r^2 + q_z^2}$ and $c = \sqrt{n/\varkappa m_0} = 1/m_0 a_0$.

The effect of coupling: change of canonical variables. Now we address the coupling between phonons and vortices. In terms of the obtained variables, the Lagrangian (103) takes on the form

$$L = \sum_k i\dot a_k a_k^\dagger + \sum_s i\dot c_s c_s^\dagger - T - H, \tag{114}$$

where $T = \int d^3r\eta\dot\Phi_0 \equiv T\{a_k, \dot a_k, a_k^\dagger, \dot a_k^\dagger, c_s, \dot c_s, c_s^\dagger, \dot c_s^\dagger\}$, and $H = H_{\rm vor} + H_{\rm ph} + H'_{\rm int}$. The coupling term T plays a special role in the Lagrangian (114). This term is linear in time derivatives of the variables and thus can not contribute to the energy in accordance with the Lagrangian formalism. Moreover, because of the time derivatives in T, the equations of motion in terms of $\{a_k, a_k^\dagger\}$, $\{c_s, c_s^\dagger\}$ take on a non-Hamiltonian form. This implies that the chosen variables become non-canonical in the presence of the interaction, and therefore the total energy, H, *in these variables* can not be identified with the Hamiltonian.

There must exist such a variable transformation $\{a_k, a_k^\dagger\}$, $\{c_s, c_s^\dagger\} \to \{\tilde{a}_k, \tilde{a}_k^\dagger\}$, $\{\tilde{c}_s, \tilde{c}_s^\dagger\}$ that restores the canonical form of the Lagrangian, $L = \sum_k i\dot{\tilde{a}}_k\tilde{a}_k^\dagger + \sum_s i\dot{\tilde{c}}_s\tilde{c}_s^\dagger - H\{\tilde{a}_k, \tilde{a}_k^\dagger, \tilde{c}_s, \tilde{c}_s^\dagger\}$. The canonical variables are obtained by the following iterative procedure. The term T is expanded with respect to $\alpha_k \ll 1$, $\beta \ll 1$ and $\eta \ll n$ yielding $T = T^{(1)} + T^{(2)} + \cdots$. Then the variables are adjusted by $a_k \to a_k + a_k^{(1)}$, $c_s \to c_s + c_s^{(1)}$, where $a_k^{(1)}(\{a_k, a_k^\dagger, c_s, c_s^\dagger\})$ and $c_s^{(1)}(\{a_k, a_k^\dagger, c_s, c_s^\dagger\})$ are chosen to eliminate the term $T^{(1)}$ in (114). As a result, $T \to 0 + T'^{(2)} + \cdots$, where the prime means that the structure of the remaining terms has changed. At the next step, $T'^{(2)}$ is eliminated by $a_k \to a_k + a_k^{(2)}$, $c_s \to c_s + c_s^{(2)}$ and so on. By construction, the canonical variables are given by $\tilde{a}_k = a_k + a_k^{(1)} + a_k^{(2)} + \cdots$, $\tilde{c}_s = c_s + c_s^{(1)} + c_s^{(2)} + \cdots$, and likewise for the conjugates. In practice, only the first few terms are enough, as the rest ones give just higher-order corrections.

The explicit expression for T is obtained following the steps of the derivation of (109). The only difference here is that the role of the auxiliary function $\boldsymbol{\rho}^2$ is played by Q, defined by $\Delta Q(\mathbf{r}) \equiv \eta(\mathbf{r})$:

$$T = 2\pi \int dz[\hat{\mathbf{z}} \times \nabla Q(\boldsymbol{\rho}_0(z), z)] \cdot \dot{\boldsymbol{\rho}}_0(z). \tag{115}$$

In accordance with $q_r\rho_0 \sim \beta k\rho_0 \ll 1$, we expand the radial functions, retaining only the greatest term for each particular angular momentum m. Switching to the cylindrical coordinates, $\boldsymbol{\rho}_0 = (\rho_0 \cos\gamma, \rho_0 \sin\gamma, 0)$, and noticing that

$$\left[\dot{\gamma}\rho_0 \frac{\partial}{\partial r} - \frac{\dot{\rho}_0}{\rho_0}\frac{\partial}{\partial\theta}\right]\mathcal{R}_{mq_r}(r)Y_m(\theta)\Big|_{r=\rho_0,\theta=\gamma} \propto \begin{cases} d(w^m)/dt, & m \geq 0, \\ d(w^{*|m|})/dt, & m < 0, \end{cases} \tag{116}$$

obtain

$$T \approx \sum_{s,k_1\ldots k_m}\left[-iA_{s,k_1\ldots k_m}c_s\frac{d}{dt}(a_{k_1}\cdots a_{k_m}) - iB_{s,k_1\ldots k_m}c_s\frac{d}{dt}(a_{k_1}^\dagger\cdots a_{k_m}^\dagger)\right] + \text{H.c.}, \tag{117}$$

where the sum is over all s with $m \neq 0$ and

$$A_{s,k_1\ldots k_m} = -\Theta(m)A_s\delta_{k_1+\cdots+k_m,-q_z},$$
$$B_{s,k_1\ldots k_m} = (-1)^{|m|}\Theta(-m-1)A_s\delta_{k_1+\cdots+k_m,q_z}, \tag{118}$$
$$A_s = \frac{\sqrt{q/m_0c}}{2^{|m|/2+1}|m|!}\frac{n^{\frac{1-|m|}{2}}(m_0\kappa)^{\frac{2-|m|}{2}}q_r^{|m|+\frac{1}{2}}q^{-2}}{L^{(|m|-1)/2}R^{1/2}},$$

where

$$\Theta(m) = \begin{cases} 1, & m \geq 0, \\ 0, & m < 0. \end{cases}$$

Thus,

$$a_k = \tilde{a}_k \tag{119}$$

(we omitted the terms that do not contain phonon operators and thus result only in relativistic corrections to the kelvon spectrum and kelvon-kelvon interactions),

$$c_s = \tilde{c}_s + (1 - \delta_{m,0}) \sum_{k_1 \ldots k_m} \Big[A_{s,k_1 \ldots k_m} \tilde{a}^\dagger_{k_1} \cdots \tilde{a}^\dagger_{k_m} + B_{s,k_1 \ldots k_m} \tilde{a}_{k_1} \cdots \tilde{a}_{k_m} \Big], \quad s = \{q_r, m, q_z\}. \tag{120}$$

The interaction Hamiltonian. The Hamiltonian H is given by the energy (104)–(106) in terms of the variables $\{\tilde{a}_k, \tilde{a}^\dagger_k\}$, $\{\tilde{c}_s, \tilde{c}^\dagger_s\}$. Up to neglected relativistic corrections, the variable transformation does not change the spectrum of the elementary modes: the zero-order Hamiltonians are given by (111), (113) in terms of $\{\tilde{a}_k, \tilde{a}^\dagger_k\}$, $\{\tilde{c}_s, \tilde{c}^\dagger_s\}$. The transform (120) applied to (113) generates the interaction term

$$H^{(\mathrm{rad})}_{\mathrm{int}} = \sum_{s,\{k_i\}} (1 - \delta_{m,0}) \Big[\omega_s A_{s,k_1 \cdots k_m} \tilde{a}^\dagger_{k_1} \ldots \tilde{a}^\dagger_{k_m} \tilde{c}^\dagger_s + \omega_s B_{s,k_1 \ldots k_m} \tilde{a}_{k_1} \cdots \tilde{a}_{k_m} \tilde{c}^\dagger_s \Big] + \mathrm{H.c.} \tag{121}$$

Remarkably, the energy term $\propto \int d^3 r \eta |\nabla \Phi_0|^2$ in (106), which results in the same as (121) operator structure, is irrelevant, being smaller in $\beta \ll 1$. It can be checked straightforwardly, that the term $\propto \int d^3 r \eta \nabla \varphi \cdot \nabla \Phi_0$ in (106) gives Fetter's amplitudes of the elastic and inelastic scattering of phonons [54] (see, however, Sect. 6.3). In addition, this term leads to a macroscopically small splitting of the phonon spectrum due to the superimposed fluid circulation.

A kelvon carries a quantum of (negative) angular momentum projection. The interaction (121) explicitly conserves the angular momentum: a real process of the emission of a phonon with the angular momentum $(-m)$ requires an annihilation of m kelvons.

6.2 Sound Emission by Kelvin-Wave Cascade

Since $\varepsilon_k \sim (a_0 k)\omega_k$, the total momentum transferred to phonons in a radiation event should be small in order to satisfy the energy conservation. Thus, the radiation by one kelvon on an infinite line is kinematically suppressed. The leading radiation process is the emission of the $m = -2$ (quadrupole) phonon mode, the events involving more than two kelvons being suppressed by $\alpha_k \ll 1$. First-order processes of the two-phonon emission come from the term $\propto \int d^3 r \eta \nabla \varphi \cdot \nabla \Phi_0$ of (106). The amplitude of these processes is suppressed by the relativistic parameter $\beta \ll 1$.

The qualitative observation that the sound emission is due to the quadrupole radiation is already sufficient to restore the formula for the power Π_k radiated by the Kelvin waves at the wavenumber scale k per unit vortex-line length. From general hydrodynamics [60], Π_k must be proportional to the square of the third-order time derivative of the quadrupole moment, $\propto \varepsilon_k^6 b_k^2 b_{-k}^2$, and inversely proportional to the fifth power of the sound velocity c. The rest of the dimensional coefficients are restored unambiguously, since the only remaining time and length scales are set by κ and k and the dimensions of mass come from the fluid density $\rho = nm_0$, which yields

$$\Pi_k \sim \frac{\kappa^2 \rho}{c^5 k} \varepsilon_k^6 b_k^2 b_{-k}^2 \sim \frac{\varepsilon_k^6 k}{c^5 \rho} n_k n_{-k}. \tag{122}$$

This result is valid up to dimensionless prefactors of order unity.

We can use the Hamiltonian (121) to obtain an accurate formula for the turbulence decay rate due to the sound radiation. The kelvon occupation number decay rate is given by $\dot{n}_k = -\sum_{s,k_1} W_{s,k,k_1}$, where W_{s,k,k_1} is the probability of the event $|0_s, n_k, n_{k_1}\rangle \to |1_s, n_k - 1, n_{k_1} - 1\rangle$ per unit time. Applying the Fermi Golden Rule to W_{s,k,k_1} with the interaction (121) and replacing the sums by integrals, obtain

$$\dot{n}_k = -\frac{(\kappa/2\pi)^5}{15\pi\rho} \left[\ln(1/a_* k) + C_0\right]^5 (k/c)^5 k^5 n_k^2. \tag{123}$$

The total power radiated by kelvons per unit vortex-line length is then obtained from $\Pi_k = -\sum_{k' \sim k} \varepsilon_{k'} \dot{n}_{k'}/L$, which allows to restore the dimensionless prefactors in (122). However, since the theories of non-structured and quasi-classical tangles can not trace coefficients of order unity we shall confine ourselves to using (122) for determining the cascade cutoff scale $\lambda_{\rm ph}$.

In both non-structured and quasi-classical tangles, at the high wavenumbers where sound radiation becomes appreciable, turbulence decay is due to the purely nonlinear Kelvin-wave cascade with the spectrum given by (53). The condition for finding the cutoff scale $\lambda_{\rm ph}$ is $\Pi_{k_{\rm ph}} \sim \theta$. Clearly, the value of θ depends on the structure of the tangle. In non-structured tangles $\theta_{\rm ns} \sim \kappa^3 \rho \Lambda^2 / l_0^2$, where l_0 is the interline separation and $\Lambda = \ln(l_0/a_*)$, which gives

$$\lambda_{\rm ph} \sim \Lambda^{24/31} \left[\kappa/c l_0\right]^{25/31} l_0 \quad \text{(non-structured tangles)}. \tag{124}$$

For the quasi-classical tangles $\theta_{\rm qc} \sim \varepsilon \rho l_0^2$, which with (76) gives $\theta_{\rm qc} \sim \kappa^3 \rho \Lambda / l_0^2 \sim \theta_{\rm ns}/\Lambda$. Thus, for the cascade cutoff we obtain

$$\lambda_{\rm ph} \sim \Lambda^{27/31} \left[\kappa/c l_0\right]^{25/31} l_0 \quad \text{(quasi-classical tangles)}. \tag{125}$$

A comment is in order here. In superfluid turbulence, kelvons do not live on infinite vortex lines, as we assumed throughout this section, but are superimposed on vortex kinks with a typical curvature radii R_0 much larger than the kelvon wavelength, $R_0 \gg k^{-1}$. This circumstance led Vinen [10] to obtain a dimensional estimate $\Pi'_k \propto b_k^2 \propto n_k$ for the power radiated per unit length of the vortex line, which is qualitatively different from our (122). In the quasi-particle language, Π'_k implies that the

radiation is governed by the conversion of *one* kelvon into a phonon. Vinen argues that this process becomes allowed in due to the finite size of the kinks, or, equivalently, the kelvon coupling to a kink lifts the ban on single-kelvon radiative processes by effectively removing the momentum conservation constraint. We note that the probabilities of such elementary events are likely to be suppressed *exponentially*, as it is generically the case, say, for soliton-phonon interactions (see, e.g., Ref. [61, 62] and references therein). The processes involving kelvon-kink coupling should contain an exponentially small factor $\sim\exp(-R_0 k)$, which arises from the convolution of the smooth kink profile with the oscillating kelvon mode.

6.3 Elastic and Inelastic Phonon Scattering

The main advantage of the Hamiltonian formalism developed here is that it allows to reduce dynamics to elementary scattering events tractable by the standard scattering theory, thereby providing a general systematic and physically transparent theoretical tool. So far, the Hamiltonian framework allowed us to address the most important remaining problems of vortex dynamics—reconnection-free kinetics of Kelvin waves and phonon radiation by Kelvin waves. The purpose of this section is to use the developed formalism to revisit the longstanding problem of phonon scattering on vortex lines. The interest to this problem has been maintained by the controversy on the value of the elastic scattering cross-section and the corresponding force between a vortex and the normal component (see Ref. [63] and references therein). The elastic scattering cross-section was originally obtained by Pitaevskii [64] and later confirmed by Sonin (Ref. [63] and references therein) basing on hydrodynamic equations of motion. However, the Hamiltonian approach to this problem suggested by Fetter [54] (and rederived later in Ref. [65]) gave a different result. Within the formalism developed in this section it is straightforward to see, as we do here by means of a direct calculation, that the discrepancy is due to the non-canonicity of the standard vortex and phonon parametrization used in the Hamiltonian of Ref. [54]. The result of Ref. [54] actually corresponds to the case of a pinned vortex, which was first noted by Sonin [63], and the effect of vortex motion during the scattering is properly accounted for by the transformation to the canonical variables.

We also discuss inelastic phonon scattering and show that the only available to our knowledge solution of Ref. [54] suffers from the same problem: the non-canonicity of the variables overlooked there makes a non-trivial contribution to the scattering cross-section. The accurate result can be obtained from a finite number of diagrams presented here (Fig. 8), but in view of the length of the resulting expression and absence of its immediate application, we do not derive it in a closed form here.

Vortex-phonon Hamiltonian in the plain-wave basis for phonon fields. For our purposes, it will be convenient to rewrite the vortex-phonon Hamiltonian of Sect. 6.1 in the plane-wave basis for the phonon fields explicitly obtaining the terms responsible for phonon scattering:

$$\begin{aligned}\eta(\mathbf{r}) &= \sum_{\mathbf{q}} \sqrt{\omega_{\mathbf{q}}\kappa/2V}\left[e^{i\mathbf{q}\mathbf{r}}c_{\mathbf{q}} + e^{-i\mathbf{q}\mathbf{r}}c^{\dagger}_{\mathbf{q}}\right],\\ \varphi(\mathbf{r}) &= -i\sum_{\mathbf{q}} \sqrt{1/2V\omega_{\mathbf{q}}\kappa}\left[e^{i\mathbf{q}\mathbf{r}}c_{\mathbf{q}} - e^{-i\mathbf{q}\mathbf{r}}c^{\dagger}_{\mathbf{q}}\right],\end{aligned} \tag{126}$$

where $\omega_{\mathbf{q}} = cq$ and $V = L^3$ is the system volume. The (harmonic part of) phonon Hamiltonian is given by (113) with s labeling different wavenumbers $\mathbf{q}$.

A calculation analogous to that of Sect. 6.1 yields the relation for the canonical variables in the form

$$a_k = \tilde{a}_k + \gamma_{kk_1\mathbf{q}}\tilde{a}_{k_1}[\tilde{c}_{\mathbf{q}} + \tilde{c}^{\dagger}_{-\mathbf{q}}] + \text{smaller terms},$$

$$\gamma_{kk_1\mathbf{q}} = -\left(\frac{q}{8Vm_0nc}\right)^{1/2}\frac{q_x^2+q_y^2}{q^2}\delta_{k_1+q_z,k}, \tag{127}$$

(we omitted the terms that do not contain phonon operators and thus result only in "relativistic" corrections to the kelvon spectrum and kelvon-kelvon interactions) and for phonon operators

$$\begin{aligned} c_{\mathbf{q}} &= \tilde{c}_{\mathbf{q}} + \sigma^*_{\mathbf{q}k}\tilde{a}_k + \sigma_{\mathbf{q}k}\tilde{a}^{\dagger}_{-k} + i\mu^*_{\mathbf{q}k_1k_2}\tilde{a}_{k_1}\tilde{a}_{k_2} + i\mu_{\mathbf{q}k_1k_2}\tilde{a}^{\dagger}_{-k_1}\tilde{a}^{\dagger}_{-k_2} \\ &\quad + \text{smaller terms}, \\ \sigma_{\mathbf{q}k} &= i(\kappa q/c)^{1/2}\frac{q_x+iq_y}{2Lq^2}\delta_{k,q_z}, \\ \mu_{\mathbf{q}k_1k_2} &= -i\frac{(q/m_0c)^{1/2}(q_x+iq_y)^2}{(32nV)^{1/2}q^2}\delta_{k_1+k_2,q_z}. \end{aligned} \tag{128}$$

Here and below we assume summation of products over repeating indices.

As in the cylindrical case, up to neglected relativistic corrections, the variable transformations (127), (128) applied to (111), (113) do not change the spectrum of the elementary modes, but generate a non-trivial contribution to the interaction Hamiltonian in higher orders:

$$\begin{aligned} H^{(1)}_{\text{int}} = \Big[& S^*_{\mathbf{q}k}\tilde{c}^{\dagger}_{\mathbf{q}}\tilde{a}_k + S_{\mathbf{q}k}\tilde{c}^{\dagger}_{\mathbf{q}}\tilde{a}^{\dagger}_{-k} + iM^*_{\mathbf{q}k_1k_2}\tilde{c}^{\dagger}_{\mathbf{q}}\tilde{a}_{k_1}\tilde{a}_{k_2} + iM_{\mathbf{q}k_1k_2}\tilde{c}^{\dagger}_{\mathbf{q}}\tilde{a}^{\dagger}_{-k_1}\tilde{a}^{\dagger}_{-k_2} \\ & + G_{kk_1\mathbf{q}}\big(\tilde{a}^{\dagger}_k\tilde{a}_{k_1}\tilde{c}_{\mathbf{q}} + \tilde{a}^{\dagger}_k\tilde{a}_{k_1}\tilde{c}^{\dagger}_{-\mathbf{q}}\big)\Big] + \text{H.c.} + \text{smaller terms}, \end{aligned} \tag{129}$$

where

$$\begin{aligned} S_{\mathbf{q}k} &= \omega_{\mathbf{q}}\delta_{\mathbf{q},\mathbf{q}'}\sigma_{\mathbf{q}'k}, \\ M_{\mathbf{q}k_1k_2} &= \omega_{\mathbf{q}}\delta_{\mathbf{q},\mathbf{q}'}\mu_{\mathbf{q}'k_1k_2}, \\ G_{kk_1\mathbf{q}} &= \varepsilon_k\delta_{k,k'}\gamma_{k'k_1\mathbf{q}}. \end{aligned} \tag{130}$$

Another relevant contribution to the interaction Hamiltonian comes from the vortex-phonon coupling energy, (106) (equivalent to the one suggested by Hall and Vinen [66, 67]),

$$H^{(2)}_{\text{int}} = \int d\mathbf{r}\eta\nabla\varphi\cdot\mathbf{v}_{\text{v}}, \tag{131}$$

where $\mathbf{v}_{\text{v}} = \mathbf{v}_{\text{v}}(\mathbf{r})$ is the velocity field produced by the vortex line. Taking into account this term alone leads to Fetter's effective interaction Hamiltonian [54] (the terms

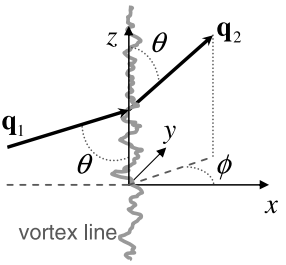

Fig. 6 Geometry of the elastic phonon scattering

$\propto \tilde{a}\tilde{c}\tilde{c}, \tilde{a}\tilde{c}^\dagger\tilde{c}^\dagger$ are omitted)

$$H_{\rm int}^{(2)} = \Big[R_{\mathbf{q_1}\mathbf{q_2}}\tilde{c}_{\mathbf{q_1}}\tilde{c}^\dagger_{\mathbf{q_2}} + R^*_{\mathbf{q_1}-\mathbf{q_2}}\tilde{c}_{\mathbf{q_1}}\tilde{c}_{\mathbf{q_2}} + T_{k\mathbf{q_1}\mathbf{q_2}}\tilde{a}^\dagger_k\tilde{c}_{\mathbf{q_1}}\tilde{c}^\dagger_{\mathbf{q_2}}\Big] + \text{H.c.} + \text{smaller terms}, \tag{132}$$

where

$$\begin{aligned} R_{\mathbf{q_1}\mathbf{q_2}} &= \frac{i\kappa}{2L^2}\sqrt{\frac{\omega_{\mathbf{q_1}}}{\omega_{\mathbf{q_2}}}}\frac{(\mathbf{q_1}\times\mathbf{q_2}\cdot\hat{\mathbf{z}})}{|\mathbf{q_1}-\mathbf{q_2}|^2}\delta_{q_1^z,q_2^z},\\ T_{k\mathbf{q_1}\mathbf{q_2}} &= \frac{1}{2V}\sqrt{\frac{\kappa L}{2m_0 n}}\mathbf{Q}_{\mathbf{q_1},\mathbf{q_2}}\cdot\Big[\hat{\mathbf{z}}\big[(\mathbf{q_2}-\mathbf{q_1})\cdot(\hat{\mathbf{x}}+i\hat{\mathbf{y}})\big] + k(\hat{\mathbf{x}}+i\hat{\mathbf{y}})\Big]\delta_{k+q_2^z,q_1^z},\\ \mathbf{Q}_{\mathbf{q_1},\mathbf{q_2}} &= \frac{(\sqrt{\frac{\omega_{\mathbf{q_2}}}{\omega_{\mathbf{q_1}}}}\mathbf{q_1}+\sqrt{\frac{\omega_{\mathbf{q_1}}}{\omega_{\mathbf{q_2}}}}\mathbf{q_2})\times(\mathbf{q_2}-\mathbf{q_1})}{|\mathbf{q_2}-\mathbf{q_1}|^2}. \end{aligned} \tag{133}$$

The complete interaction Hamiltonian up to the highest relevant order in $\beta \ll 1$, $\alpha_k \ll 1$, and $|\eta|/n \ll 1$ is given by $H_{\rm int} = H_{\rm int}^{(1)} + H_{\rm int}^{(2)}$. Note that in this form the Hamiltonian conservers the momentum along the vortex line (along the z-axis), but not the transverse momentum. The change of transverse momentum during the scattering is transferred to the vortex line as a whole (an analog of the Mössbauer effect), which results in a macroscopically small displacement of the vortex line from its initial position. The corresponding Goldstone mode can be straightforwardly taken into account if necessary.

Elastic phonon scattering. We consider the scattering geometry shown in Fig. 6. The vortex line has a distribution of kelvon occupation numbers $\{n_k\}$. The elastic scattering differential cross-section can be found as

$$\frac{d\sigma}{d\phi} = (V/c)\frac{d}{d\phi}\sum_{\mathbf{q_2}} W_{\mathbf{q_1}\to\mathbf{q_2}}, \tag{134}$$

where $W_{\mathbf{q_1}\to\mathbf{q_2}}$ is the probability per unit time of a scattering event of a phonon with the wavenumber $\mathbf{q_1}$ into the one with $\mathbf{q_2}$, such that $\mathbf{q_1} = q_1(\sin\theta, 0, \cos\theta)$, $\mathbf{q_2} = q_2(\sin\theta\cos\phi, \sin\theta\sin\phi, \cos\theta)$. The probability $W_{\mathbf{q_1}\to\mathbf{q_2}}$ is given by the Golden rule,

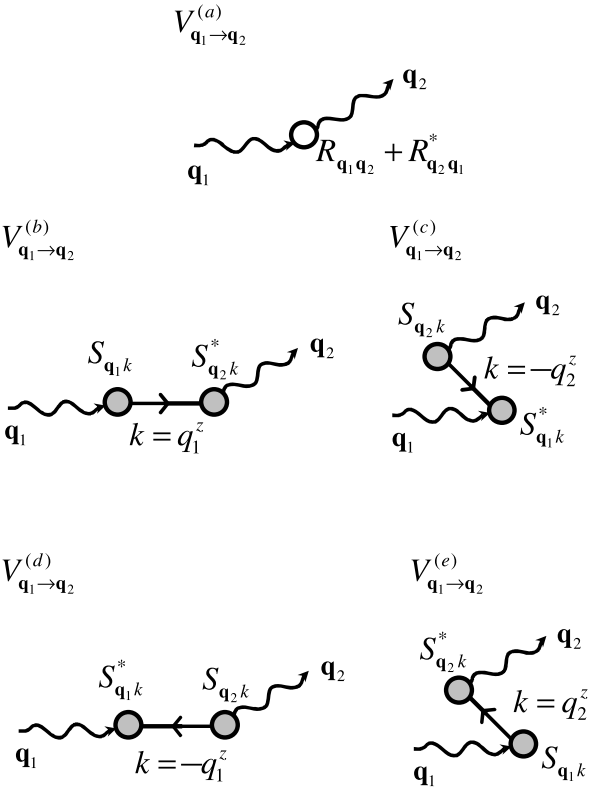

Fig. 7 Diagrammatic representation of the transition amplitude of elastic phonon scattering on a vortex line. The *wavy* and *straight lines* represent phonons and kelvons respectively

$W_{\mathbf{q}_1\to\mathbf{q}_2} = 2\pi\delta(\omega_{\mathbf{q}_1} - \omega_{\mathbf{q}_1})|V_{\mathbf{q}_1\to\mathbf{q}_2}|^2$. To the first (Born) approximation the transition amplitude $V_{\mathbf{q}_1\to\mathbf{q}_2}$ is composed of the elementary processes shown diagrammatically in Fig. 7. Note that, in Ref. [54] only the term $V^{(a)}_{\mathbf{q}_1\to\mathbf{q}_2}$ was taken into account. The remaining terms describe a scattering process in which the vortex line undergoes a virtual deformation (produced by a kelvon with $k = q_{1z}$). It is easily seen that physically $V^{(b-e)}_{\mathbf{q}_1}$ account for the oscillatory motion of the vortex line induced during the scattering: if the vortex were pinned by an external potential these terms would have to vanish. The transition amplitudes in Fig. 7 are given by

$$V^{(a)}_{\mathbf{q}_1\to\mathbf{q}_2} = R_{\mathbf{q}_1\mathbf{q}_2} + R^*_{\mathbf{q}_2\mathbf{q}_1} = \frac{i\kappa}{2L^2}\frac{\sqrt{q_1 q_2}(q_1+q_2)\sin^2\theta\sin\phi}{q_1^2+q_2^2-2q_1q_2(\sin^2\theta\cos\phi+\cos^2\theta)}\delta_{q_1^z,q_2^z}, \tag{135}$$

$$V^{(b)}_{\mathbf{q}_1\to\mathbf{q}_2} = \frac{S_{\mathbf{q}_1 k}S^*_{\mathbf{q}_2 k}}{\omega_q - \varepsilon_k}(n_k+1), \tag{136}$$

$$V^{(c)}_{\mathbf{q}_1\to\mathbf{q}_2} = \frac{S_{\mathbf{q}_2 k}S^*_{\mathbf{q}_1 k}}{-\omega_q - \varepsilon_k}(n_{-k}+1), \tag{137}$$

$$V^{(d)}_{\mathbf{q}_1\to\mathbf{q}_2} = \frac{S_{\mathbf{q}_2 k} S^*_{\mathbf{q}_1 k}}{\omega_q + \varepsilon_k} n_{-k}, \tag{138}$$

$$V^{(e)}_{\mathbf{q}_1\to\mathbf{q}_2} = \frac{S_{\mathbf{q}_1 k} S^*_{\mathbf{q}_2 k}}{-\omega_q + \varepsilon_k} n_k. \tag{139}$$

Note, that at small scattering angles the amplitude $V^{(a)}_{\mathbf{q}_1\to\mathbf{q}_2}$ diverges and the perturbation theory is not applicable. However, the small-angle scattering does not play an important role for the dissipative component of the mutual friction force. Since $\varepsilon_k/\omega_q \sim a_0 q_{1z} \lesssim \beta \ll 1$ for $|k| = |q_{1z}| = |q_{2z}|$, we can neglect the kelvon energy in the denominators of (135)–(139). Thus, the terms proportional to $\{n_k\}$ cancel out in the total transition amplitude,

$$V_{\mathbf{q}_1\to\mathbf{q}_2} = R_{\mathbf{q}_1\mathbf{q}_2} + \left[S_{\mathbf{q}_1 k} S^*_{\mathbf{q}_2} - \text{c.c.}\right]/\omega_q, \tag{140}$$

meaning that alternatively the amplitude can be obtained by retaining only the terms of type $V^{(a-c)}_{\mathbf{q}_1\to\mathbf{q}_2}$ but evaluating them in kelvon vacuum. Substituting the vertex expressions into (140) and doing the algebra yields

$$V_{\mathbf{q}_1\to\mathbf{q}_2} = \frac{i\kappa}{2L^2} \frac{\sin^2\theta \sin\phi\cos\phi + \cos^2\theta \sin\phi}{1-\cos\phi} \delta_{q_{1z},q_{2z}}. \tag{141}$$

Finally, replacing the sum in (134) by the integral,

$$\frac{d\sigma}{d\phi} = (V/c) \int \frac{q_2\, dq_2 L^2}{2\pi} \delta(\omega_{\mathbf{q}_1} - \omega_{\mathbf{q}_1}) |V_{\mathbf{q}_1\to\mathbf{q}_2}|^2, \tag{142}$$

we arrive at

$$\frac{d\sigma}{d\phi} = Lq \frac{\kappa^2}{8\pi c^2} \frac{[\sin^2\theta \sin\phi\cos\phi + \cos^2\theta \sin\phi]^2}{(1-\cos\phi)^2}. \tag{143}$$

For $\theta = \pi/2$ this result gives the differential cross-section obtained in Ref. [63]. Due to the divergency at $\phi \to 0$, this formula is only applicable in the cases where the small-angle scattering is irrelevant, as, e.g., in a calculation of the dissipative mutual friction force, which immediately follows from (143). In contrast, the calculation of the non-dissipative component is essentially non-perturbative and is discussed in Ref. [63].

Inelastic scattering. Employing the same formalism, we describe the inelastic phonon scattering, i.e. scattering accompanied by generation of Kelvin waves. In the diagrammatic language the transition amplitude $V_{\mathbf{q}_1\to\mathbf{q}_2,k}$, where k is the kelvon wavenumber, is shown in Fig. 8. Note that the extra diagrams with reversed propagators are dropped, which is accounted for by evaluating the remaining ones over kelvon vacuum. The scattering matrix element reported in Ref. [54] corresponds to the first term $\propto T_{k\mathbf{q}_1\mathbf{q}_2}$ only.

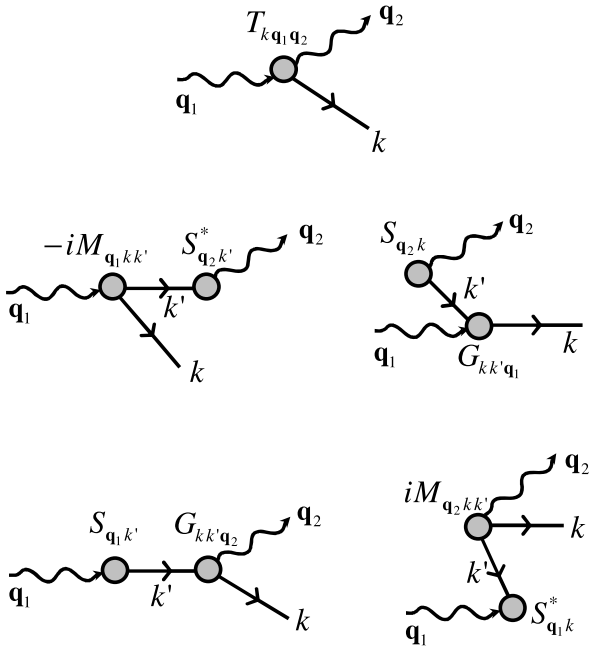

Fig. 8 Inelastic phonon scattering. The diagrams give the total transition amplitude. The *wavy* and *straight lines* represent phonons and kelvons respectively. The virtual kelvons are described by vacuum propagators

7 Conclusions and Discussion

The zero-temperature limit of superfluid turbulence is non-trivial and instructive. A number of small and large parameters—(1), (30), (98)—and (approximately) conserving quantities (energy, momentum, number of kelvons, LIA constants of motion), characterizing the phenomenon, bring about rich physics on one hand, and provide a solid basis for applicability of the analytic tools on the other.

The central part in the theory is played by the large parameter Λ, (1). Implications of the condition $\Lambda \gg 1$ include (i) universality of the answers for all U(1)-type superfluids, (ii) applicability of LIA, (iii) features following from (ii), of which the most important ones are (a) the integrability of LIA suppressing the efficiency of the pure Kelvin-wave cascade and (b) preemptive character of the self-induced motion of the vortices in the smallest Richardson-Kolmogorov eddies, responsible for cutting off the classical-fluid regime *before* it could experience a potential bottleneck associated with (a).

The energy and momentum conservation renders impossible the pure vortex ring cascade (originally proposed by Feynman) in which superfluid turbulence is supposed to decay into small rings in such a way that each ring produces smaller ones independently of the rest of the vortex tangle. The absence of pure Feynman's cascade and suppressed efficiency of the pure Kelvin-wave cascade create specific circumstances under which there exists a range in the kelvon wavenumber space—with the size controlled by Λ—where the Kelvin-wave cascade is driven by this or that type of vortex line reconnections. The reconnections lift the integrability constraint of the LIA and push the vortex-line length to higher and higher wavenumbers.

In the theoretical limit of really large Λ (to be taken with a grain of salt in view of realistic $\Lambda \lesssim 15$ in ^{4}He), we predict three distinct types of reconnection-driven Kelvin-wave cascades. The first two ones (in the down-the-cascade order)—(i) vortex-bundle-reconnection-based and (ii) neighboring-line-reconnection-based—apply only to the Richardson-Kolmogorov quasi-classical regime, while the third one, driven by local self-crossings, applies to non-structured tangles as well, including superfluid turbulence sustained by vibrating objects. At large-enough wavenumbers, the local-self-crossings-driven cascade naturally crosses over to the pure Kelvin-wave cascade, as soon as the power of the latter becomes sufficient to compete with the former, eventually suppressing the reconnections by rendering the amplitude of Kelvin waves small compared to their wavelength.

At $T = 0$, the inertial range of the pure Kelvin-wave cascade is controlled by the small parameter β, defined in (98), that guarantees irrelevance of compressibility and/or kelvon-phonon interaction before the cascade reaches the wavelength scale $\lambda \sim \lambda_{\rm ph}$, where phonon emission becomes dominant, cutting the cascade off. In a typical case, $1/\beta \gg \Lambda \sim \ln(1/\beta)$, implying that the inertial range of the pure Kelvin-wave cascade is significantly larger than that of the reconnection-driven cascade(s).

Kinetics of the pure Kelvin-wave cascade are perturbative due to the asymptotically vanishing amplitude-to-wavelength ratio. This allows one to introduce a kinetic equation with the collision term associated with kelvon scattering. Because of the conservation of the total number of kelvons (which is nothing but the conservation of the angular momentum) and one-dimensional character of the problem, the leading kinetic process is the elastic three-kelvon scattering. As an effect of the LIA integrability constraint, the kinetics are entirely due to the interactions going beyond the LIA: the local contributions to the effective three-kelvon scattering amplitude exactly cancel each other leaving no order-Λ collision terms and suppressing kinetic rates.

The small amplitude of Kelvin waves at the dissipative cutoff wavenumbers and weak kelvon-phonon coupling guaranteed by the parameter β imply that the phonon emission is a perturbative process that can be naturally described within the Hamiltonian formalism. Our derivation of the kelvon-phonon Hamiltonian revealed a subtlety of non-canonicity of the prime harmonic variables with respect to the interaction Hamiltonian. Adequately accounting for this fact at the level of hydrodynamic action leads to a proper kelvon-phonon interaction Hamiltonian, containing terms that would be missed otherwise. With this Hamiltonian the problem of the phonon cutoff of the Kelvin-wave cascade becomes rather straightforward. The leading process is two-kelvon inelastic scattering converting two kelvons with almost opposite momenta into one phonon. As a by-product, we resolved some long-standing controversies of the kelvon-phonon interaction, showing that these were due to the above-mentioned lacking terms in the interaction Hamiltonian. (We also revealed the role of a hidden phonon-vortex interaction in the theory of Berezinskii-Kosterlitz-Thouless transition [68], which is not covered here.)

Having at hand a complete theoretical scenario for superfluid turbulence at $T = 0$, it is important to check it against experiment and numeric simulations. Discussing first the more simple case of non-structured turbulence, we note that a circumstantial evidence for the Kelvin-wave cascade—the absence of temperature dependence of the turbulence relaxation time—has been observed in both experiment [7] (although the absolute temperature scale reported there is rather questionable, see, e.g.,

Ref. [31]) and simulations [9]. The simulation of Ref. [9], performed within LIA (and after Ref. [5] was published), could potentially identify the local self-crossings driven cascade. Moreover, the authors did observe production of vortex rings. However, they interpreted that as the pure Feynman's cascade. A direct numeric support for the local self-crossing scenario can be found in Ref. [17], where the behavior of a vortex line attached to a vibrating object was studied within the LIA. It was observed that as a response to the external perturbation the vortex line gets kinky, after which frequent local self-crossings result in a systematic production of vortex rings.

Still very desirable is a simulation of the zero-temperature decay of non-structured turbulence within the full Biot-Savart description. Such a simulation could quantify our very rough order-of-magnitude estimate of the crossover between local-self-crossing-driven and pure Kelvin-wave cascades and answer the fundamental question of whether the inertial range of the cascade of self-crossings is large enough for realistic $\Lambda \lesssim 15$ to be taken seriously in the experimental context.

Turning now to the Richardson-Kolmogorov regime, we emphasize the recent experimental progress [18] that allowed to probe the vortex line length as a function of temperature. As we discussed in Sect. 5, the experiment is in a very good qualitative agreement with our crossover scenario, the observed pronounced increase of the vortex line length at friction coefficient $\sim 10^{-3}$ being indicative of the line fractalization. Nevertheless, it is still a circumstantial rather than direct evidence. A direct experimental evidence for the local self-crossings driven scenario might be an observation of small vortex rings emitted by spatially localized Richardson-Kolmogorov superfluid turbulence.

On the theoretical side, a simulation of the crossover from Richardson-Kolmogorov to Kelvin-wave regime might be very instructive, especially given that numerically one can set Λ to be arbitrarily large to render the role of this parameter more pronounced. Yet another missing theoretical piece—in view of only an order-of-magnitude estimate and a technical mistake in our Ref. [13], mentioned in Sect. 3—is an accurate result for the numerical prefactor in the energy flux of the pure Kelvin-wave cascade, (43).

Summarizing our results for the crossover from Richardson-Kolmogorov to Kelvin-wave regime, we cannot leave without a discussion the work by L'vov, Nazarenko, and Rudenko [19], which triggered our interest to the problem. As discussed in Sect. 5, the authors of Ref. [19] put forward an idea of bottleneck accumulation of energy in the wavenumber space between the classical-field hydrodynamic modes and Kelvin waves. The notion of bottleneck in Ref. [19] is unequivocally defined as being associated with the absence of *any* channel capable of accommodating the energy flux produced by the Richardson-Kolmogorov cascade, which implies *thermalization* of hydrodynamic modes in a certain range of length scales *above* the Kelvin-wave regime. In our Ref. [20] (see also Sect. 5), we pointed out that this idea is inconsistent with the above-mentioned preemptive role of reconnections as an energy transport mechanism. While agreeing with us [21][2] on the importance of the

[2]In the revised version of their manuscript, the authors of Ref. [19] admit potential importance of the self-induced motion, referring to the preprint of our Ref. [20].

self-induced motion of vortices in the smallest—of the size $\sim r_0$ defined in (75)—Richardson-Kolmogorov eddies, and attempting to revise their theory accordingly in Ref. [21], the same authors still insist on unimportance of reconnections and support the bottleneck idea. Note, however, that once we start from the grounds that the self-induced motion dominates vortex-line dynamics, reconnections are unavoidable—the lines simply do not interact with each other, and thus there is nothing to stop them from coming into a direct contact and reconnecting. We explicitly demonstrate in Sect. 5 that these reconnections serve as an efficient channel of transferring the energy flux to lower scales thereby ruling out a possibility of the bottleneck.

In a certain loose sense, term 'bottleneck' might be associated with the phenomenon of fractalization of vortex lines (cf. Ref. [18]), since it is essentially an accumulation of energy in some region of the inertial range. We, however, see two reasons—one specific to the context of superfluid turbulence and, most importantly, a generic fundamental one—why doing so could be misleading. The specific reason is that the term has been already used in the context of the interface between hydrodynamic and Kelvin-wave modes, while fractalization of the lines is a purely Kelvin-wave effect, which happens deep (in the $\Lambda \to \infty$ limit) in the quantized regime. The fundamental reason is that the fractalization of the lines does not at all imply the absence of a channel(s) capable to accommodate the energy flux—the fractalization starting at a given wavelength scale does not result in any back action on larger scales, such as the development of a thermalized distribution above the bottleneck, which is a crucial ingredient of bottleneck scenarios. A more relevant term, putting the effect of vortex line fractalization in a broader context of exotic cascade phenomena, might be the *deposition* of the cascading constant of motion (e.g., energy in our case) within the cascade inertial range. While re-distributing the cascading quantity in a non-trivial way along the inertial range, the effect of deposition does not plug the cascade, thus leaving its generic properties intact.

References

1. R.J. Donnelly, *Quantized Vortices in He II* (Cambridge University Press, Cambridge, 1991)
2. C.F. Barenghi, R.J. Donnelly, W.F. Vinen (eds.), *Quantized Vortex Dynamics and Superfluid Turbulence*. Lecture Notes in Physics, vol. 571 (Springer, Berlin, 2001)
3. W.F. Vinen, J.J. Niemela, J. Low Temp. Phys. **128**, 167 (2002)
4. W.F. Vinen, J. Low Temp. Phys. **145**, 7 (2006)
5. B.V. Svistunov, Phys. Rev. B **52**, 3647 (1995)
6. C. Nore, M. Abid, M.E. Brachet, Phys. Rev. Lett. **78**, 3896 (1997)
7. S.I. Davis, P.C. Henry, P.V.E. McClintock, Physica B **280**, 43 (2000)
8. W.F. Vinen, Phys. Rev. B **61**, 1410 (2000)
9. M. Tsubota, T. Araki, S.K. Nemirovskii, Phys. Rev. B **62**, 11751 (2000)
10. W.F. Vinen, Phys. Rev. B **64**, 134520 (2001)
11. D. Kivotides, J.C. Vassilicos, D.C. Samuels, C.F. Barenghi, Phys. Rev. Lett. **86**, 3080 (2001)
12. W.F. Vinen, M. Tsubota, A. Mitani, Phys. Rev. Lett. **91**, 135301 (2003)
13. E.V. Kozik, B.V. Svistunov, Phys. Rev. Lett. **92**, 035301 (2004)
14. E.V. Kozik, B.V. Svistunov, Phys. Rev. Lett. **94**, 025301 (2005)
15. E. Kozik, B. Svistunov, Phys. Rev. B **72**, 172505 (2005)
16. D.I. Bradley, D.O. Clubb, S.N. Fisher, A.M. Guénault, R.P. Haley, C.J. Matthews, G.R. Pickett, V. Tsepelin, K. Zaki, Phys. Rev. Lett. **96**, 035301 (2006)
17. R. Hanninen, M. Tsubota, W.F. Vinen, Phys. Rev. B **75**, 064502 (2007)

18. P.M. Walmsley, A.I. Golov, H.E. Hall, A.A. Levchenko, W.F. Vinen, Phys. Rev. Lett. **99**, 265302 (2007)
19. V.S. L'vov, S.V. Nazarenko, O. Rudenko, Phys. Rev. B **76**, 024520 (2007)
20. E. Kozik, B. Svistunov, Phys. Rev. B **77**, 060502 (2008)
21. V.S. L'vov, S.V. Nazarenko, O. Rudenko, J. Low Temp. Phys. **153**, 140 (2008)
22. E. Kozik, B. Svistunov, Phys. Rev. Lett. **100**, 195302 (2008)
23. P.M. Walmsley, A.I. Golov, Phys. Rev. Lett. **100**, 245301 (2008)
24. S.Z. Alamri, A.J. Youd, C.F. Barenghi, Phys. Rev. Lett. **101**, 215302 (2008)
25. C.F. Barenghi, Physica D **237**, 2195 (2008)
26. S.K. Nemirovskii, Phys. Rev. B **77**, 214509 (2008)
27. M. Blaûková, D. Schmoranzer, L. Skrbek, W.F. Vinen, Phys. Rev. B **79**, 054522 (2009)
28. G. Boffetta, A. Celani, D. Dezzani, J. Laurie, S. Nazarenko, arXiv:0810.3573v1
29. S.K. Nemirovskii, arXiv:0902.3720v1
30. E.A.L. Henn, J.A. Seman, G. Roati, K.M.F. Magalhaes, V.S. Bagnato, Phys. Rev. Lett. (2009, to appear). arXiv:0904.2564v2
31. A.I. Golov, P.M. Walmsley, J. Low Temp. Phys. (2009). doi:10.1007/s10909-009-9896-9
32. W.F. Vinen, Proc. R. Soc. Lond., Ser. A **240**, 114 (1957)
33. W.F. Vinen, Proc. R. Soc. Lond., Ser. A **242**, 493 (1957)
34. W.F. Vinen, Proc. R. Soc. Lond., Ser. A **243**, 400 (1957)
35. K.W. Schwarz, Phys. Rev. B **31**, 5782 (1985)
36. K.W. Schwarz, Phys. Rev. B **38**, 2398 (1988)
37. J. Maurer, P. Tabeling, Europhys. Lett. **43**, 29 (1998)
38. S.R. Stalp, L. Skrbek, R.J. Donnelly, Phys. Rev. Lett. **82**, 4831 (1999)
39. S.R. Stalp, J.J. Niemela, W.F. Vinen, R.J. Donnelly, Phys. Fluids **14**, 1377 (2002)
40. T.V. Chagovets, A.V. Gordeev, L. Skrbek, Phys. Rev. E **76**, 027301 (2007)
41. N.G. Berloff, B.V. Svistunov, Phys. Rev. A **66**, 013603 (2002); and references therein
42. C.N. Weiler, T.W. Neely, D.R. Scherer, A.S. Bradley, M.J. Davis, B.P. Anderson, Nature **455**, 948 (2008)
43. T.W.B. Kibble, J. Phys. A **9**, 1387 (1976)
44. W.H. Zurek, Nature **317**, 505 (1985)
45. S.V. Iordanskii, Z. Eksp. Teor. Fiz. **49**, 225 (1965) (Sov. Phys. JETP **22**, 160 (1966))
46. R.P. Feynman, in *Progress in Low Temperature Physics*, vol. 1, ed. by C.J. Gorter (North-Holland, Amsterdam, 1955), p. 17
47. R. Betchov, J. Fluid Mech. **22**, 471 (1965)
48. H. Hasimoto, J. Fluid Mech. **51**, 477 (1972)
49. V.E. Zakharov, S.V. Manakov, S.P. Novikov, L.P. Pitaevskii, *Theory of Solitons* (Nauka, Moscow, 1980)
50. R.I. Epstein, G. Baym, Astrophys. J. **387**, 276 (1992)
51. B.V. Svistunov, J. Mosc. Phys. Soc. **1**, 373 (1991)
52. T.F. Buttke, J. Comput. Phys. **76**, 301 (1988)
53. D.C. Samuels, R.J. Donnelly, Phys. Rev. Lett. **65**, 187 (1990)
54. A.L. Fetter, Phys. Rev. **186**, 128 (1969) and references therein
55. V. Bretin, P. Rosenbush, F. Chevy, G.V. Shlyapnikov, J. Dalibard, Phys. Rev. Lett. **90**, 100403 (2003)
56. T. Mizushima, M. Ichioka, K. Machida, Phys. Rev. Lett. **90**, 180401 (2003)
57. J.-P. Martikainen, H.T.C. Stoof, Phys. Rev. A **69**, 053617 (2004)
58. E.M. Lifshitz, L.P. Pitaevskii, *Statistical Mechanics, Part 2* (Pergamon Press, New York, 1980)
59. V.N. Popov, *Functional Integrals in Quantum Field Theory and Statistical Physics* (Reidel, Dordrecht, 1983)
60. E.M. Lifshitz, L.P. Pitaevskii, *Fluid Mechanics* (Pergamon Press, New York, 1987)
61. G. Reinisch, J.C. Fernandez, Phys. Rev. B **25**, 7352 (1982)
62. K. Maki, Phys. Rev. B **26**, 2181 (1982)
63. E.B. Sonin, Phys. Rev. B **55**, 485 (1997)
64. L.P. Pitaevski, Z. Eksp. Teor. Fiz. **35**, 1271 (1958) (Sov. Phys. JETP **8**, 888 (1959))
65. E. Demircan, P. Ao, Q. Niu, Phys. Rev. B **52**, 476 (1995)
66. H.E. Hall, W.F. Vinen, Proc. Roy. Soc., Ser. A **238**, 204 (1956)
67. H.E. Hall, W.F. Vinen, Proc. Roy. Soc., Ser. A **238**, 215 (1956)
68. E. Kozik, N. Prokof'ev, B. Svistunov, Phys. Rev. B **73**, 092501 (2006)